

CHAPTER III

DIELECTRIC INVESTIGATIONS OF LIQUID CRYSTALLINE MATERIALS EXHIBITING DIFFERENT TYPES OF SMECTIC A-NEMATIC TRANSITIONS

3.1 INTRODUCTION

In a nematic liquid crystal there is long range orientational order of the geometrically anisotropic molecules, while the centres of mass are distributed at random as in an ordinary isotropic fluid. Smectic liquid crystals have stratified structures, but different types of molecular arrangement are possible within each stratification. The simplest of these is the smectic A phase in which the molecules are upright with their centres irregularly spaced in a liquid-like fashion. McMillan¹ has extended the Maier-Saupe theory to include an additional order parameter for characterizing the translational periodicity of such a layered structure. McMillan¹ and Kobayashi² showed theoretically that the nematic-smectic A (N-A) transition could be first or second order.

The dielectric behaviour of liquid crystals is determined by the permanent dipoles and molecular polarizability. Because of the uniaxial symmetry in nematic and smectic A liquid crystals the dielectric permittivity differs in value along the preferred

axis (ϵ_{\parallel}) and perpendicular to this axis (ϵ_{\perp}). Maier and Meier³ have extended Onsager's theory⁴ for isotropic liquids to the case of nematic liquid crystals. Their equations account satisfactorily for many essential features of the permittivity of nematic liquid crystals. According to this theory, the dielectric anisotropy,

$$\Delta\epsilon = \epsilon_{\parallel} - \epsilon_{\perp} = \frac{4\pi N\rho hF}{M} \left[\Delta\alpha - \frac{F\mu^2}{2k_B T} (1 - 3\cos^2\beta) \right] S,$$

where $h = [3\bar{\epsilon}/(2\bar{\epsilon}+1)]$ represents the cavity field factor, $\bar{\epsilon} = (\epsilon_{\parallel} + 2\epsilon_{\perp})/3$ the mean dielectric constant, $F = 1/(1 - \bar{\alpha}f)$ the reaction field factor, $\bar{\alpha}$ the mean polarizability, $f = [4\pi N\rho(2\bar{\epsilon} - 2)]/[3M(2\bar{\epsilon} + 1)]$, ρ the density, M the molecular weight, N the Avagadro number, μ the permanent dipole moment, β the angle that the permanent dipole moment makes with respect to the long molecular axis, k_B the Boltzmann constant, S the nematic order parameter and $\Delta\alpha$ the polarizability anisotropy.

The idea of near neighbour antiparallel correlations (or anti-ferroelectric short range order) in nematic liquid crystals composed of polar molecules was first proposed by Madhusudana and Chandrasekhar⁵ and its consequences were discussed on the basis of the Bethe-Peierls cluster approximation. A prediction of this theory is that the mean dielectric constant $\bar{\epsilon}$ should show a discontinuous increase on going from the nematic to the isotropic phase. This

has been experimentally verified for a number of cyano mesogens.⁶ Another consequence of near neighbour correlation is the formation of the bilayer smectic A phase. The existence of such a bilayer phase in materials consisting of strongly polar end group was proved experimentally by Xray and neutron scattering experiments of Leadbetter et al.^{7,8} Thus a partially bilayer phase wherein the thickness of the layer is more than the length of the molecule was established. However the richness of polymorphism of smectic A phase became obvious only after the pioneering work of the Bordeaux group. Sigaud et al.⁹ while studying the binary phase diagram of 4-n-pentylphenyl-4'-cyanobenzoyloxybenzoate/terephthal bis-4-n-butylaniline (DB5CN/TBBA) observed a phase transition between two types of smectic A phases. Although optical studies failed to show any difference in the textures exhibited by the two A phases, calorimetric studies showed a clear signature of the smectic A-smectic A transition. Thus the first smectic A-smectic A transition was found. Xray studies^{1,} conducted on oriented samples showed that the higher temperature phase was the monolayer phase with layer spacing (d) approximately equal to the length of the molecule (R). In this way this phase is similar to the monolayer phase observed in materials without any strongly polar end group, the existence of which in symmetric molecules has been known for a long time. The lower temperature phase

in the DB5CN/TBBA system showed an interesting X-ray diffraction pattern. It showed two condensed X-ray reflections — one corresponding to the layer spacing equal to the length of the molecule ($d=l$) and the other corresponding to twice the length of the molecule ($d=2l$) and hence it was designated as the bilayer phase (A_2 phase). This discovery of Sigaud et al.⁹ opened a new field of experimental and theoretical study. Subsequent studies¹¹⁻¹⁴ have shown the existence of three more types of smectic A phases, viz., the antiphase (\tilde{A}), the crenellated A phase (A_{cre}) and the most recently discovered incommensurate A phase (A_{ic}).

The schematic diagrams depicting the molecular arrangement in different types of smectic A phases are given in Fig. 3.1. As already discussed the monolayer phase is characterised by $d \approx l$, the dipoles within the layer being randomly distributed. To this extent the structure of the monolayer phase composed of molecules with a strongly polar end group is closely similar to that of the smectic A phase exhibited by materials whose molecules are terminally non-polar. For the sake of convenience of discussion, hereafter we shall be referring to the former type of smectic A phase as polar A_1 phase and the latter type of A phase as non-polar A_1 phase.

Fig.3.1 also shows that the molecules in the partially

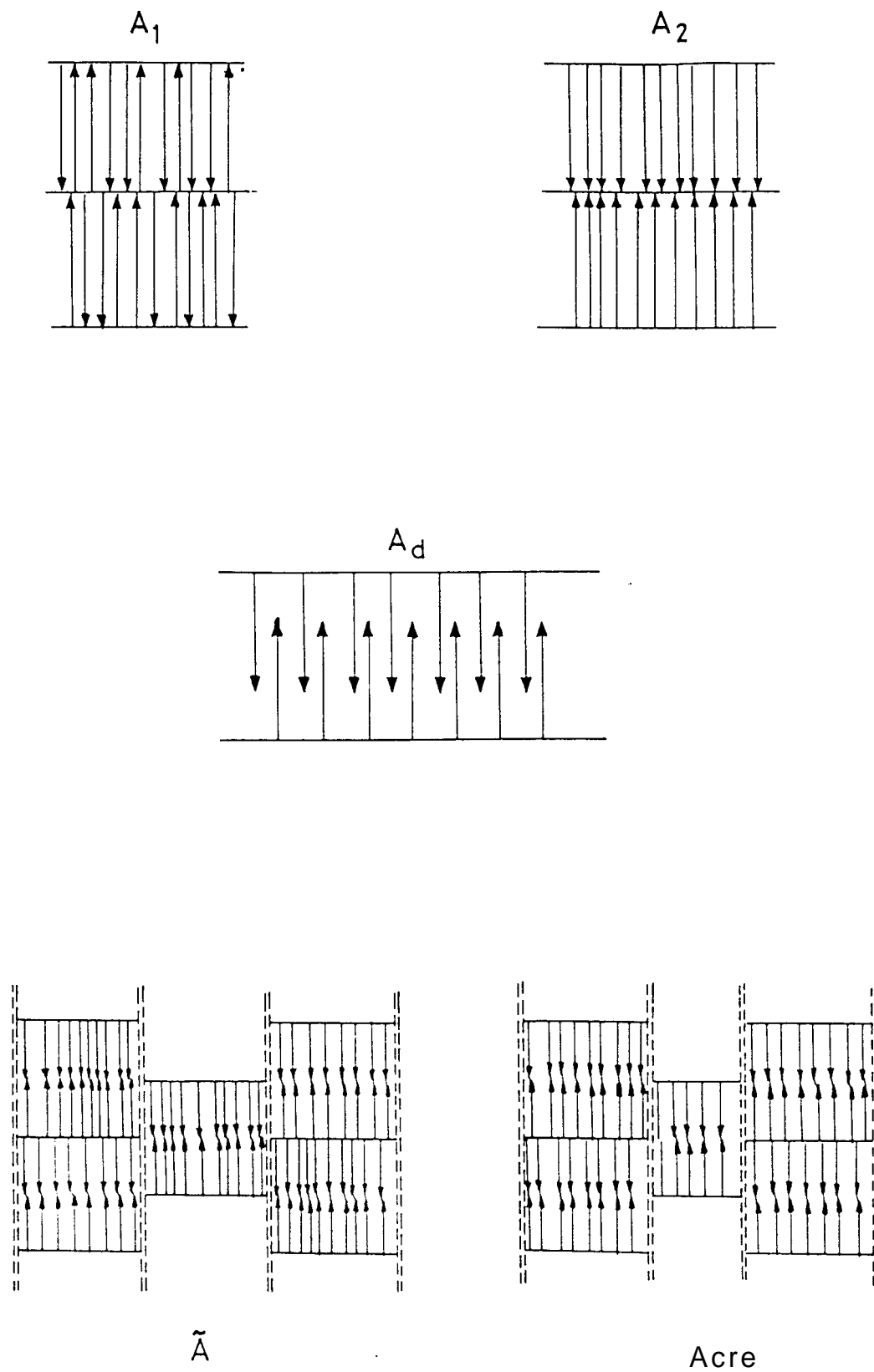


Figure 3.1

Schematic representation of the molecular arrangement in the different A phases.

bilayer phase (A_D phase) are interdigitated. The extent of interdigitation depends on the material. Most of the polar materials whose dielectric properties were studied earlier^{6,15-21} exhibit the A_D phase. In case of the bilayer phase (A_2 phase) the molecules are supposed to be arranged in a head-to-head configuration as shown in figure 3.1. The antiphase (\tilde{A}) has essentially the same local symmetry as of the A_2 phase but there is a significant difference. In the case of the \tilde{A} phase, groups of dipoles are arranged in either up or down configuration so that one can look upon the structure as consisting of a "dipolar wave" within the layer. The molecular picture of the A_{iC} phase has not yet been established.

All the molecular pictures described above have been postulated on the basis of Xray diffraction patterns exhibited by monodomain samples of A phases. Since it is well known from earlier studies⁶ that near-neighbour antiparallel correlations of strongly polar molecules are manifested in their dielectric properties, it is important to study the behaviour of dielectric properties near different kinds of N-A transitions and to see if the dielectric behaviour can be correlated to the structural differences between the different A phases. This chapter describes the results of our investigations taken up on materials exhibiting different types of N-A transitions.

32 MATERIALS

The different materials whose nematic-smectic A (N-A) transitions have been studied are listed in Table 3.1 along with the transitions exhibited by them and their temperatures. The structural formulae of these materials are given in Fig.3.2.

For the study of N-polar A_1 transition, three materials belonging to 4-(4'-alkoxybenzoyloxy)-4'-cyanoazobenzenes (nOBCAB) series have been used, viz., 4-(4'-butoxybenzoyloxy)-4'-cyanoazobenzene (4OBCAB), 4-(4'-hexyloxybenzoyloxy)-4'-cyanoazobenzene (6OBCAB) and 4-(4'-octyloxybenzoyloxy)-4'-cyanoazobenzene (8OBCAB). Interestingly these nOBCAB compounds^{22,23} were in fact amongst the first to show the reentrant nematic phase and polymorphism of A phases. The transition temperatures versus chain length plot for the homologous series of nOBCAB is shown in fig.3.3. It is seen that the N- A_1 transition temperature is a maximum for n=6. The second type of A phase, viz., the A_d phase is exhibited by the n=9 and n=10 homologues, a reentrant nematic phase intervening between the A_d and A_1 phases for these homologs.

The material chosen to study a typical N-nonpolar A_1 transition is 4-n-heptyloxy - phenyl-4-n-decyloxybenzoate (7OPDOB). A number of studies have already been reported on materials exhibiting such a transition.²⁴⁻³⁰

TABLE 3.1

The sequences and the temperatures of transitions of
the compounds studied

S.No.	Compound	Transition temperatures (in °C)			
		<u>K - A₁ (or N)</u>	<u>A₁ - N</u>	<u>N - I</u>	
1	4(4'-alkoxybenzoyloxy)-4'- cyano azobenzene (nOBCAB) (Polar A ₁)	n = 4	110.2	108.3	297.0
		n = 6	107.4	127.0	275.2
		n = 8	92.8	99.0	257.5
2	4-n-heptyloxy-phenyl 4-n- decyloxy benzoate (7OPDOB) (Non-polar A ₁)	<u>K - C</u>	<u>C - A₁</u>	<u>A₁ - N</u>	<u>N - I</u>
		69.7	80.2	84.2	87.8
3	4-cyanobenzylidene-4'-n- octyloxyaniline (CBOOA) (A _d)	<u>K - A_d</u>	<u>A_d - N</u>	<u>N - I</u>	
		73.0	82.8	107	
4	4-n-pentyl phenyl-4'-cyano benzoyloxy benzoate (DB5CN) (A ₂)	<u>K - A₂</u>	<u>A₂ - N</u>	<u>N - I</u>	
		127	139.5	249	

K : Crystal

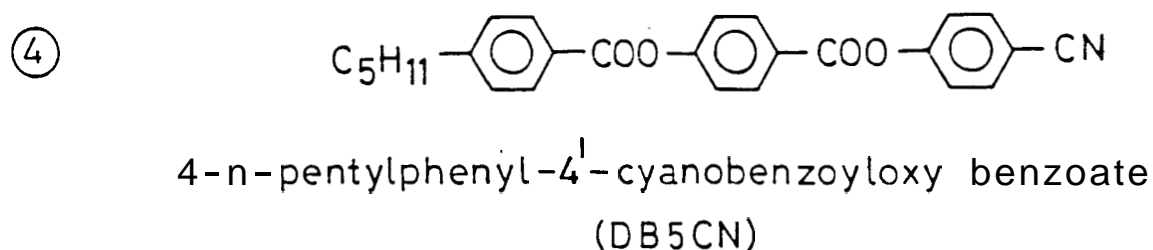
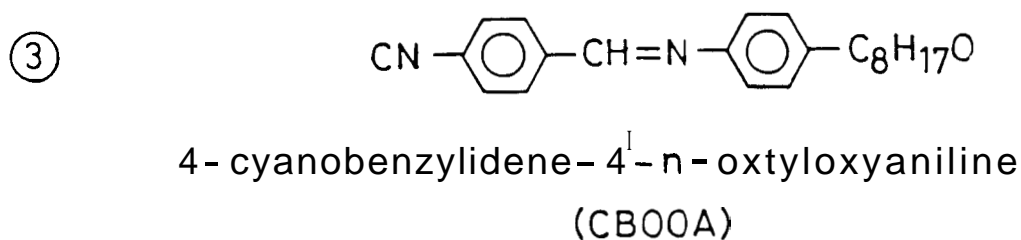
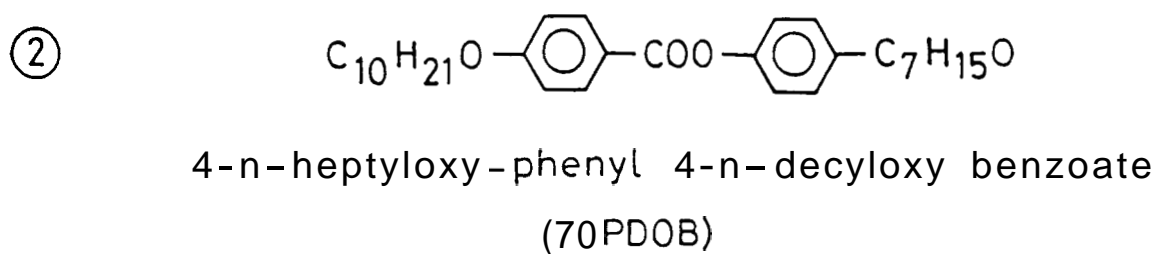
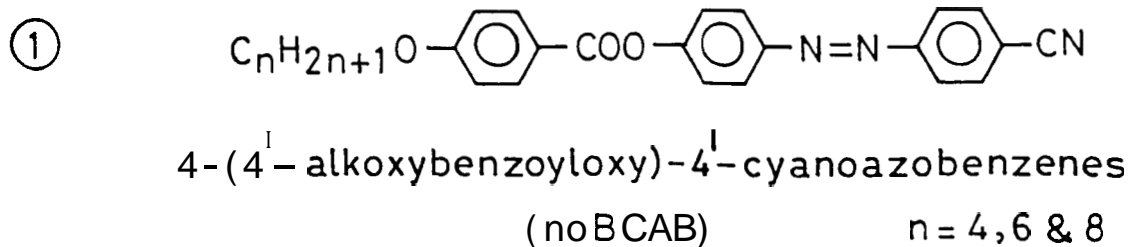


Figure 3.2

The structural formulae and the abbreviations used for the compounds studied

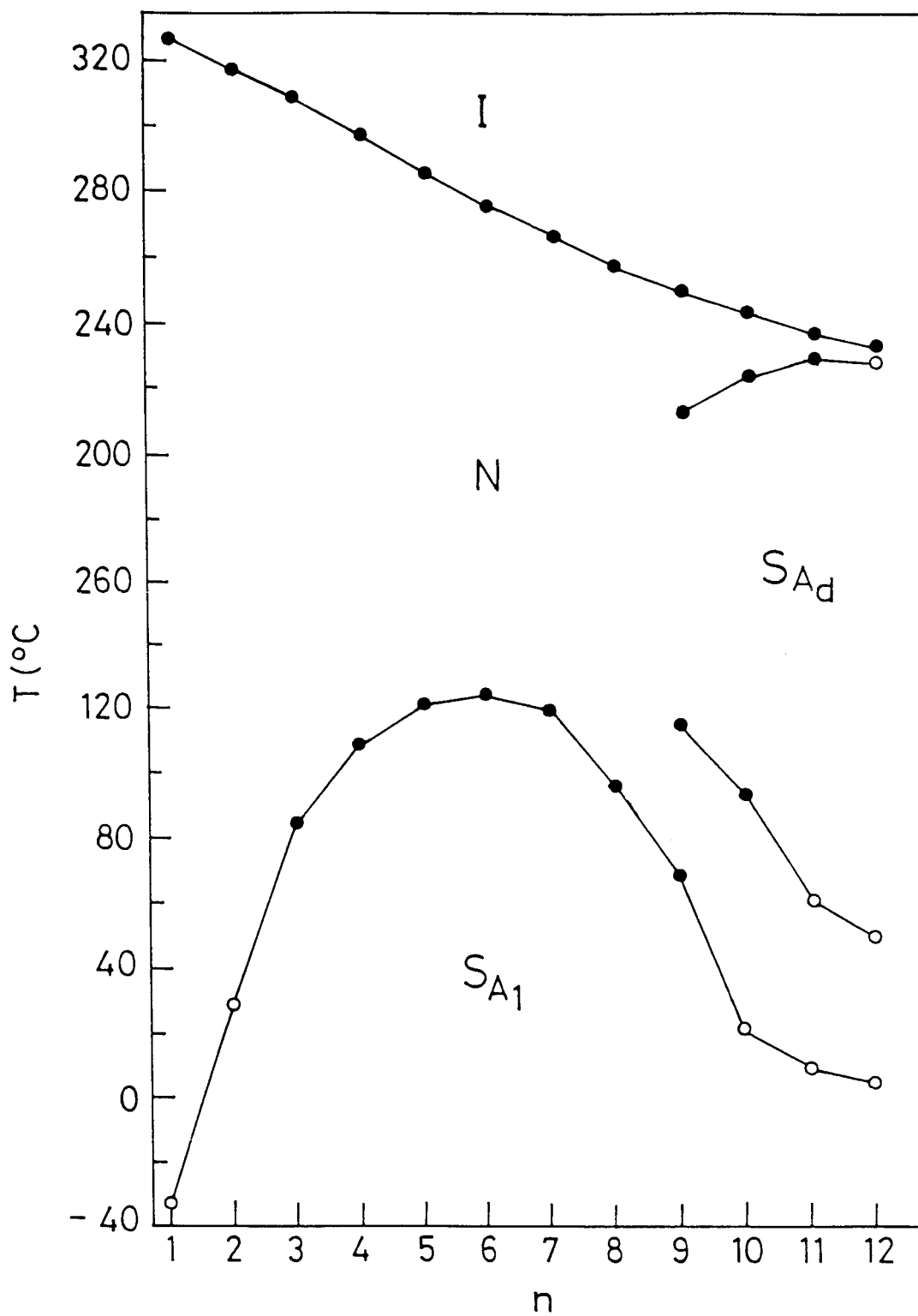


Figure 3.3

Plot showing transition temperature (●) vs. chain length for the 4-alkoxybenzoyloxy-4'-cyanoazobenzene series; (○) are extrapolated values (From Ref. 22).

In the case of the N-A_d transition, the material used for dielectric study is 4-cyanobenzylidene-4'-n-octyloxyaniline (CBOOA). The N-A_d transition in CBOOA has been the subject of a variety of experimental studies.³¹ Initially the N-A_d transition in this material was considered to be first order.³² However subsequent high resolution experiments have clearly shown that this transition is second order.³³

The most recently discovered⁹ N-A transition is the N-A₂ transition. Very few materials are known which exhibit this kind of transition. We have studied this transition in 4-n-pentylphenyl-4'-cyanobenzoyloxybenzoate (DB5CN) which is in fact the first material in which such a transition was discovered.

3.3 EXPERIMENTAL

3.3.1. Xray Studies

Xray diffraction data^{8,10,34} on some of the materials discussed in the preceding section are already available. However on some others, e.g., the nOBCAB materials, no such data is available and thus it was necessary to conduct an Xray study on these compounds. The experimental set up used in this study is described in the following:

The samples were taken in Lindemann glass capillary tubes

and the ends of the tubes were sealed. The experiments were conducted on magnetically oriented samples using monochromatic CuK_α radiation obtained from a Xray generator (Philips PW1730) in conjunction with a bent quartz crystal monochromator (Carl Zeiss, Jena). The diffracted Xray beam was recorded on a flat photographic film which was located at the focus of the monochromator. The constancy of temperature during any exposure was $\pm 0.1^\circ\text{C}$. The distance between the diffraction spots on the film was measured using a precision comparator (Adam-Hilger Ltd.). The relative accuracy in the determination of d is reckoned to be $\pm 0.1\%$

3.3.2 Dielectric Studies

a) Static.

The details of the experimental set up used has already been given in Chapter II. The dielectric constants were measured using a Hewlett-Packard Impedance Analyser (HP4192A). As mentioned earlier, for the experiments described in this chapter, the data were collected manually. The thickness of the sample used was $50\ \mu\text{m}$ and it was aligned in the nematic phase by a 2.4 Tesla magnetic field and cooled very slowly into the A phase in the presence of this field. The static measurements were carried out at 1 KHz and the temperature was varied very slowly ($\sim 4^\circ\text{C/hr}$) near the transition.

b) Dispersion

The low frequency relaxation of ϵ_{\parallel} was measured using the same set up mentioned in the earlier section. During dispersion study, the temperature of the sample was maintained constant to within ± 25 mK. At any temperature the values of $\epsilon_{\parallel}^{\prime}$ and $\epsilon_{\parallel}^{\prime\prime}$ were measured as functions of frequency.

3.4 N TO A₁ (NON-POLAR) TRANSITION

In this section, we shall describe the results of our study on 7OPDOB which exhibits N, A and C phases, the transition temperatures being given in Table 3.1.

3.4.1 Static Dielectric Constants

The variation of static dielectric constants ϵ_{\parallel} and ϵ_{\perp} as well as of the dielectric anisotropy $\Delta\epsilon$ with temperature (T) are shown in Figs. 3.4 and 3.5 respectively. The compound has a negative $\Delta\epsilon$ throughout the N and A phases (no data in the C phase is given since it was not possible to get a planar alignment in this phase). As the material is cooled from the isotropic phase, ϵ_{\perp} increases with decrease in temperature while ϵ_{\parallel} decreases. The rate of decrease of ϵ_{\parallel} is much steeper than the rate of in-

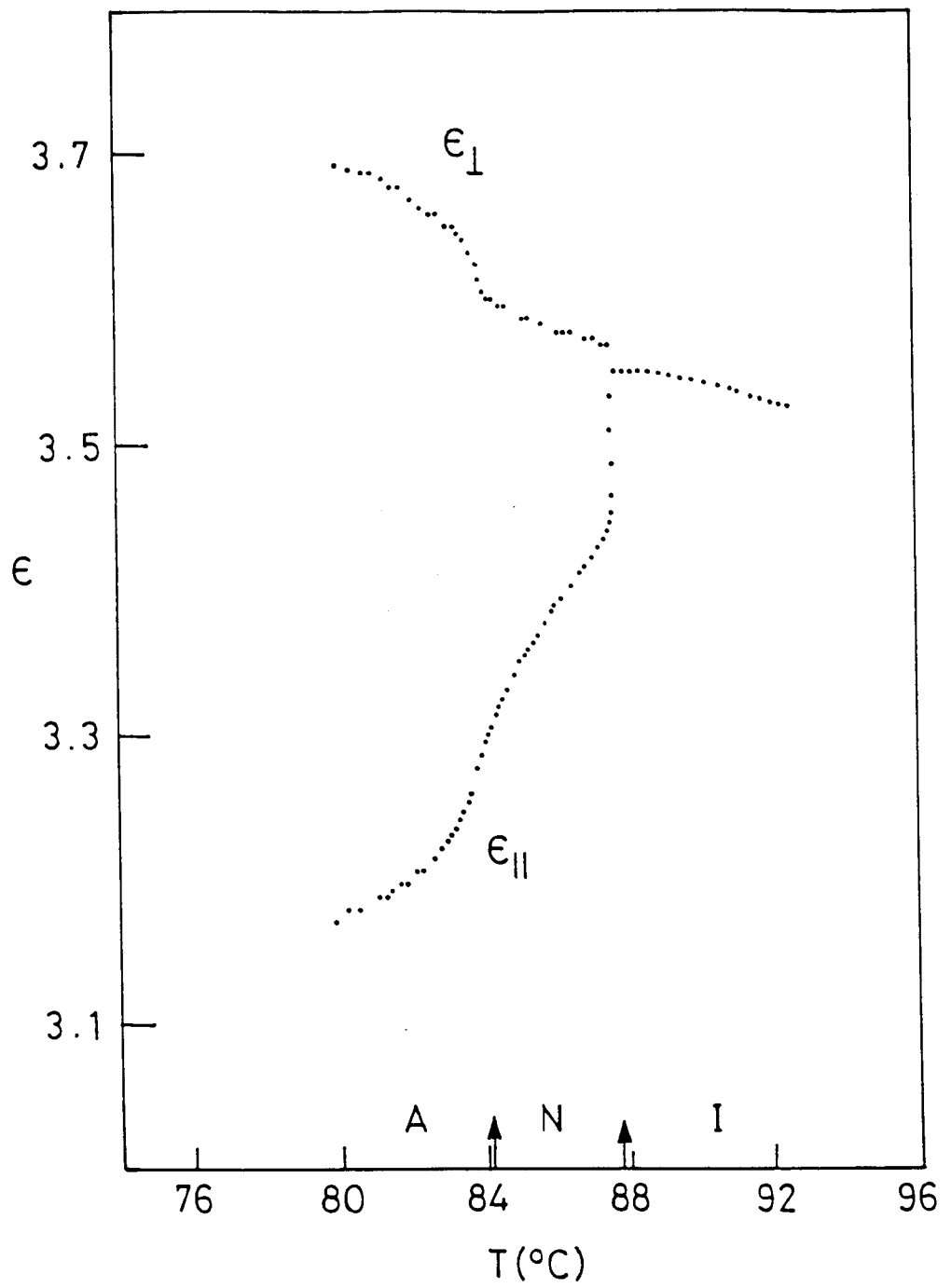


Figure 3.4

The temperature variation of the dielectric constants ϵ_{\parallel} and ϵ_{\perp} in the isotropic, nematic and smectic A phases of 7OPDOB.

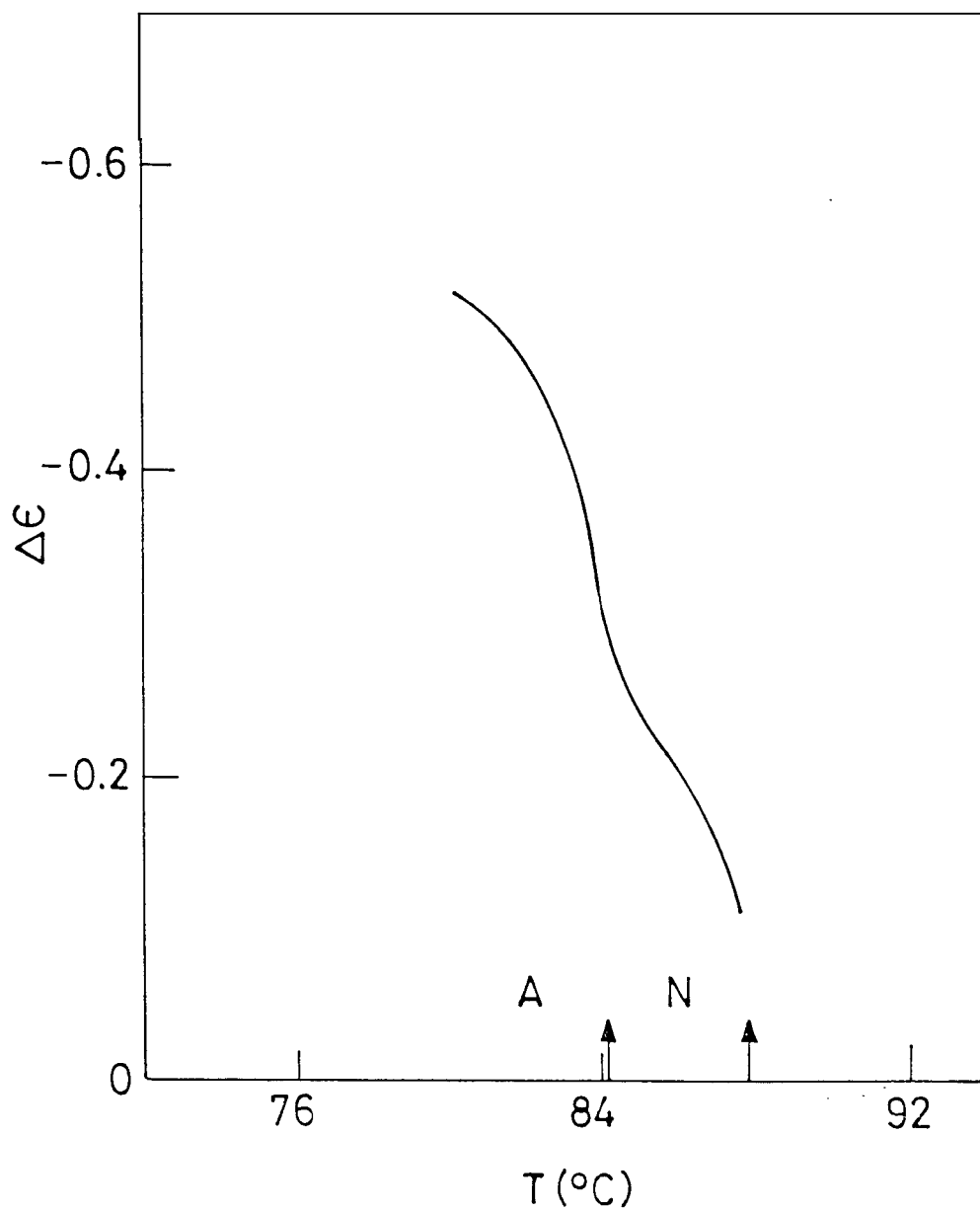


Figure 3.5

The temperature variation of the dielectric anisotropy, $\Delta\epsilon$ for 7OPDOB.

crease of ϵ_{\perp} . The steep decrease in ϵ_{\parallel} could perhaps be due to enhanced dipole-dipole correlation in the longitudinal direction. This could also be of course due to Maier-Meier equation³ which has the $1/T$ factor. The signature of the N-A transition is the change in the slope in both ϵ_{\parallel} and ϵ_{\perp} . No breaks could be seen in either ϵ_{\parallel} or ϵ_{\perp} within the resolution of our experimental set up. In the smectic A phase, ϵ_{\perp} continues to increase while ϵ_{\parallel} decreases. It is clear from Fig.3.5 that $\Delta\epsilon$ varies steeply throughout N and A phases with a conspicuous change in slope at N-A transition. These results are essentially similar to those on the lower members of the same homologous series, viz., 6OPDOB and 5OPDOB.^{24,27,28,30} The anisotropy of 7OPDOB is found to be similar to that of the other homologs.

3.4.2 Dispersion

We shall now present the low frequency ϵ_{\parallel} relaxation studies on 7OPDOB. Since it was possible to get homeotropic alignment, we have been able to make dispersion measurements in all the three phases, viz., N, A and C phases. As remarked earlier, during dispersion measurements, the temperature was kept constant to better than ± 25 mK and the capacitance (C) and the dielectric loss factor (D) were measured as functions of frequency in the measuring range of the instrument (5 Hz-13 MHz). Care was taken to collect more data in the neighbourhood of the dispersion fre-

quency. Typical curves of dielectric loss, viz., ϵ''_{\parallel} versus frequency curves in N, A and C phases are shown in Fig.3.6. It is clear that the dispersion is well characterized with a sharp maximum in the loss curve. The position of the maximum gives the frequency of relaxation f_R . This was determined graphically. The determination of f_R from the loss curve obtained in this manner is expected to be accurate to about 2%. Representative Cole-Cole plots in N,A and C phases are given in Fig.3.7. It is clear that there is a single relaxation process in all the phases. The data fit a semi-circle very well with the centre lying on the ϵ'_{\parallel} axis. The relaxation frequency is also obtained from such Cole-Cole plots, again graphically. Table 3.2 gives the complete data on f_R obtained for a series of temperatures in the N, A and C phases both by loss curves and by Cole-Cole plots. The average value of f_R determined by the two techniques is plotted versus $1/T$ in Fig.3.8. From the slope, the activation energy W , associated with the reorientation of the longitudinal component of the dipole moment about the short axis is calculated. The values of W evaluated in this manner in N, A and C phases are also marked in the same figure. It is clear that the activation energy in the nematic phase is greater than the activation energy in the A phase which in turn is greater than the energy in the C phase ($W_N > W_A > W_C$).

Buka and Bata²⁷ have measured the dielectric dispersion

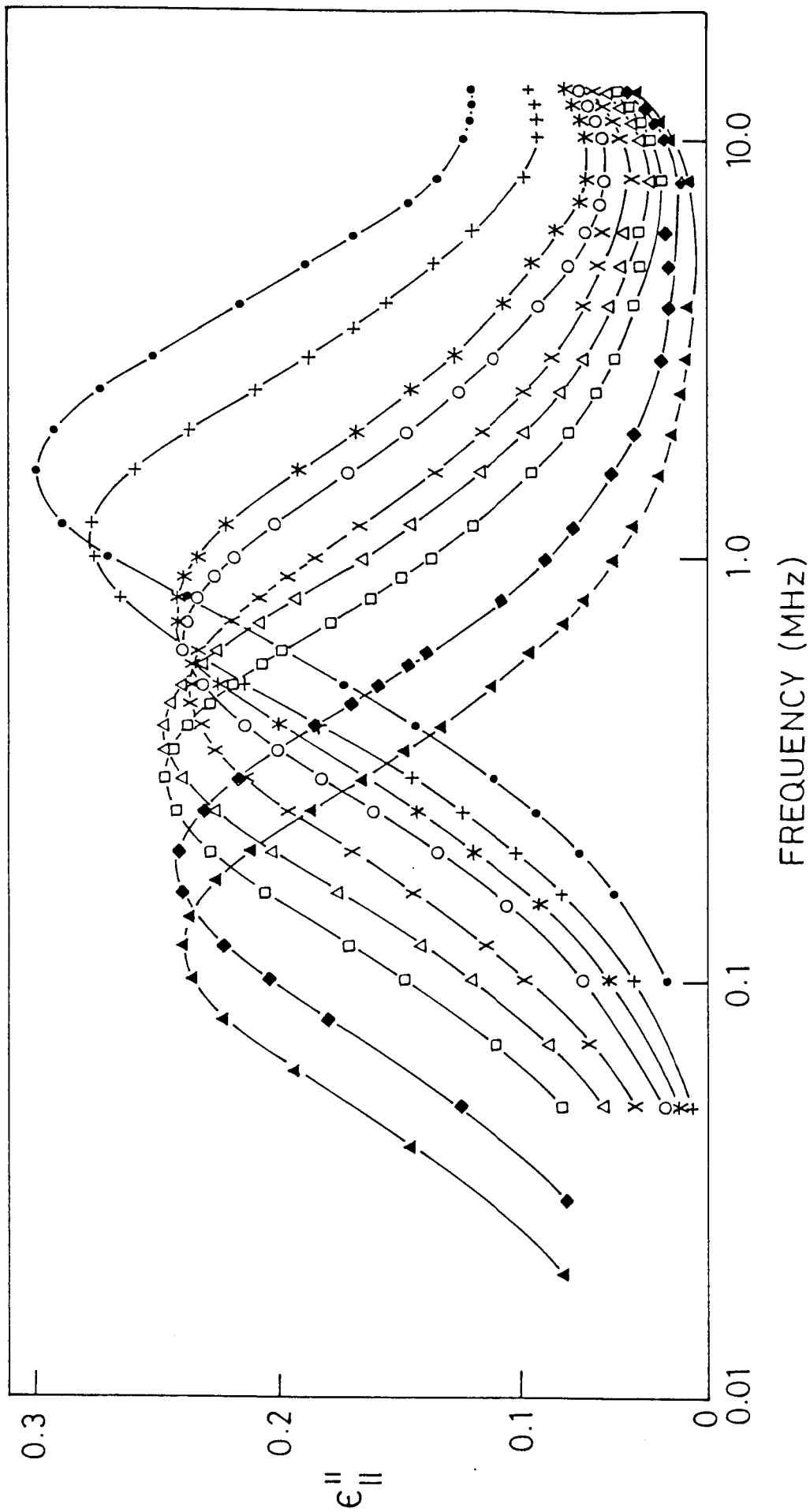


Figure 3.6. The representative loss curves of 70PDOB in the (a) nematic (● 86.5°C, † 85.4°C, * 84.5°C), (b) smectic A₁ (○ 83.6°C, X 81.9°C, Δ 80.7°C) and (c) smectic C phase (◻ 79°C, ◆ 75°C, ▲ 71.4°C).

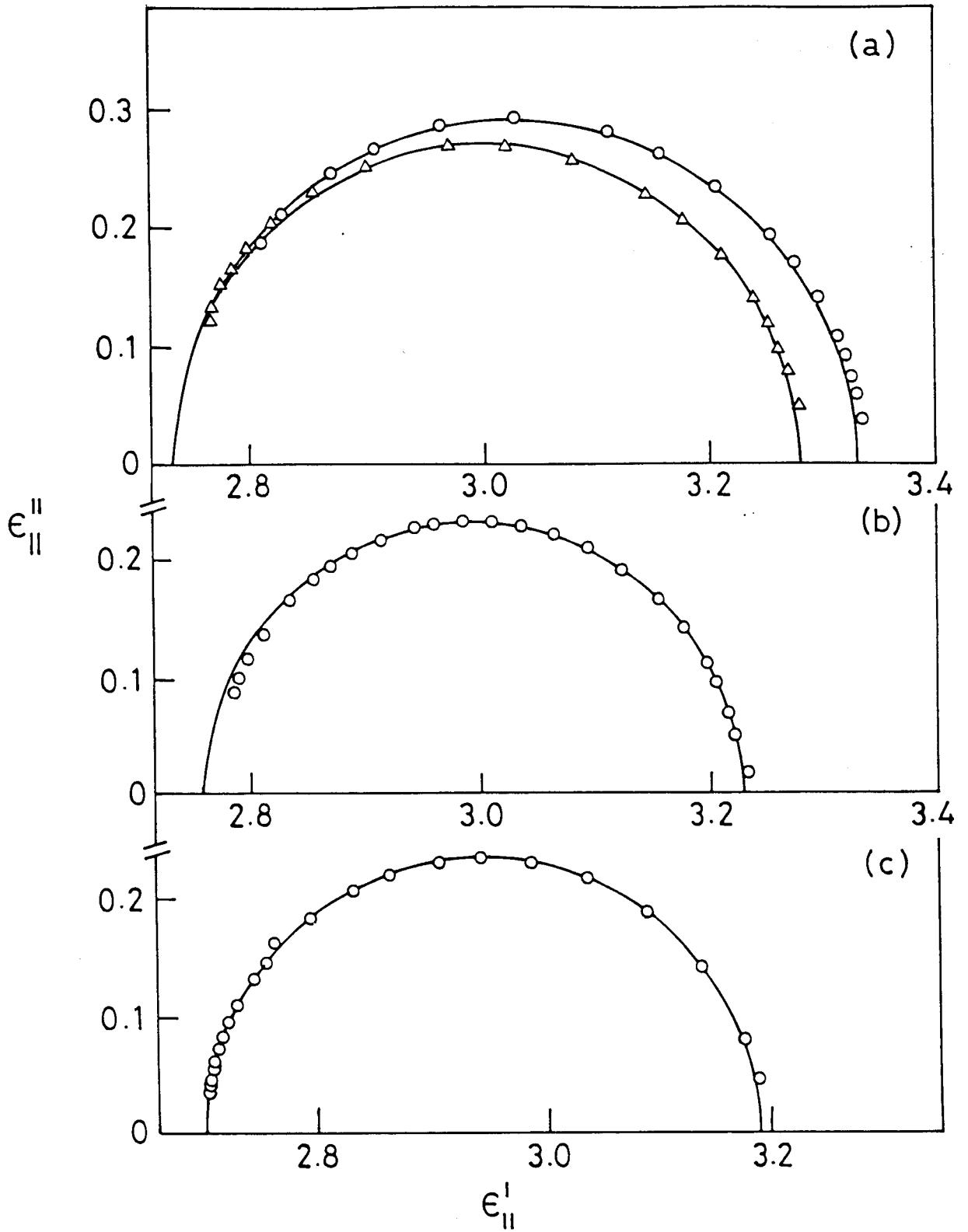


Figure 3.7

Representative Cole-Cole plots in the (a) nematic (\circ 86.5°C, \triangle 85.4°C), (b) smectic A_1 (81.9°C) and (c) smectic C (71.4°C) phases of 70PDOB.

TABLE 3.2

Frequency of relaxation f_R as a function of temperature in
N, smectic A and C phases for 7OPDOB

S. No.	Temperature (°C)	Frequency of Relaxation (in MHz)		
		From loss curve	From Cole-Cole	Mean f_R
<u>N e m a t i c</u>				
1	86.5	1.6	1.59	1.595
2	86.0	1.38	1.37	1.375
3	85.4	1.1	1.08	1.09
4	85	0.890	0.882	0.886
5	84.5	0.765	0.764	0.765
<u>S m e c t i c A</u>				
6	83.6	0.660	0.670	0.665
7	82.7	0.560	0.555	0.558
8	81.9	0.475	0.474	0.475
9	81.2	0.418	0.420	0.419
10	80.7	0.385	0.381	0.383
<u>S m e c t i c C</u>				
11	79	0.297	0.298	0.298
12	78	0.262	0.260	0.261
13	76.7	0.225	0.226	0.226
14	75	0.182	0.183	0.183
15	72.9	0.139	0.140	0.140
16	71.4	0.120	0.120	0.120

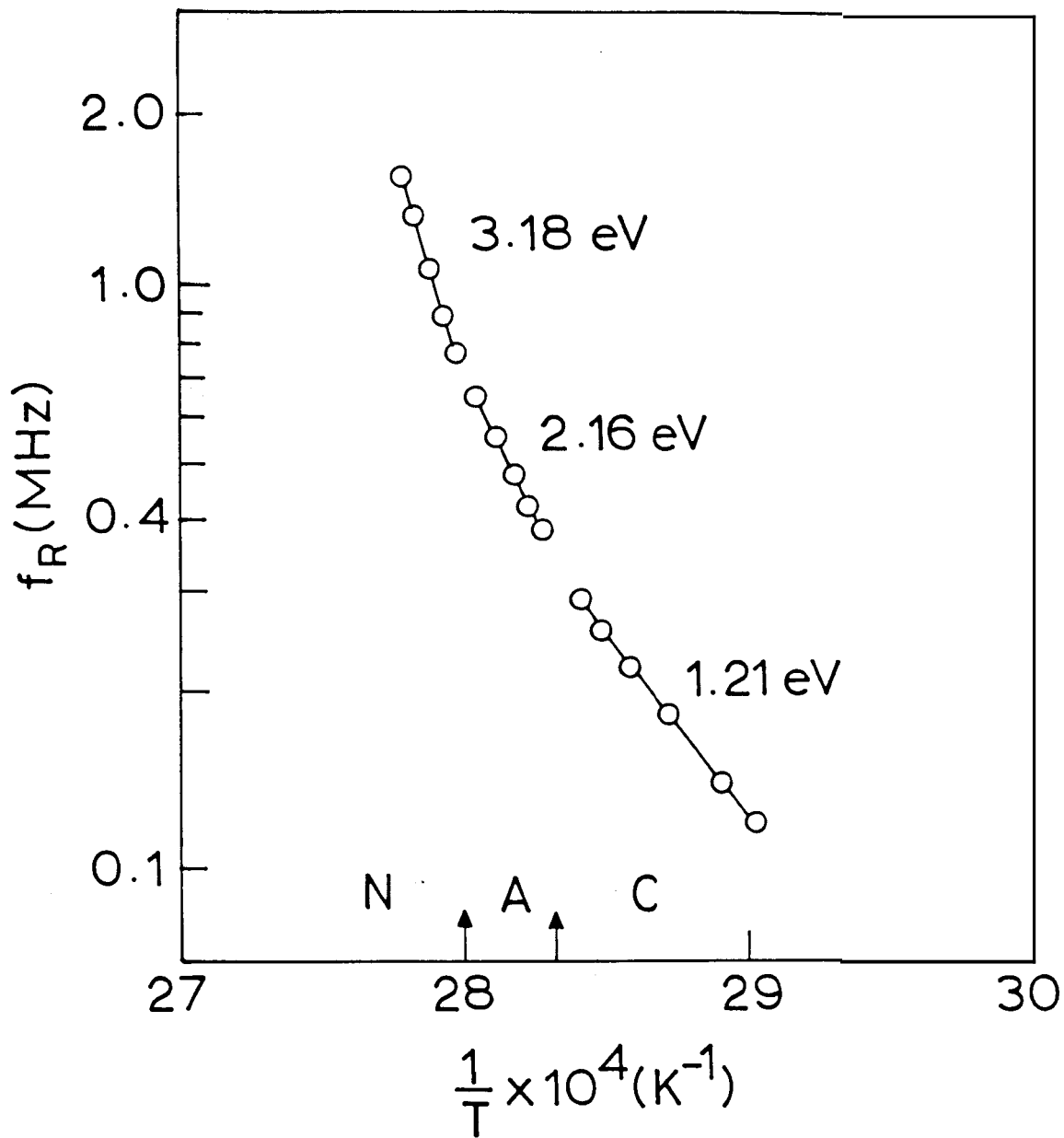


Figure 3.8

The plot of the relaxation frequency f_R versus $1/T$ of 70PDOB. The activation energies are also shown.

in 6OPDOB, a lower homologue of 7OPDOB. They have also found $W_N > W_A > W_C$ in agreement with our observation on 7OPDOB (see table 3.3). In fact the values of W for the 2 compounds are similar. Buka and Bata have further shown that in the C phase, which is not a uniaxial system, the relaxation around the short axis can have two modes, one measured along the layer normal and the other perpendicular to it. The relaxation frequencies for these two modes coincide for the corresponding temperatures. However the intensity of absorption decreases with decrease of temperature in the first case while the reverse is true in the second case. We believe that we have measured the relaxation frequency in mode 1 since in our case the strength of the absorption decreases with decrease of temperature.

In summary it is clear that the low frequency relaxation process in both nematic and monolayer A phases of terminally non-polar material 7OPDOB is characterized by highest activation energy in N phase and lowest in C phase. This result by itself cannot be explained by any existing theories^{35,36} since the activation energy (W), associated with molecular reorientation about short axis, consists of contribution due to nematic potential and viscosity. Since the A phase has higher orientational order as well as higher viscosity, one would expect that W in N phase should be less than in A phase. However 7OPDOB shows that it is not

TABLE 33

The activation energy W corresponding to the low frequency of relaxation obtained in the nematic, smectic A and C phases for different compounds

Material	Activation Energy (in eV)			Reference
	Nematic	Smectic A	Smectic C	
6OPDOB	3.22	1.97	1.29	Buka and Bata ²⁷
7OPDOB	3.18	2.16	1.21	This work

the case. In fact most of the materials whose dielectric properties are studied so far^{17-20,29,37,38} show this theoretically ununderstood behaviour. This problem has been reviewed recently by Chandrasekhar.³⁹

3.5 NEMATIC-SMECTIC A_1 (POLAR) TRANSITION

We have discussed earlier the dielectric behaviour near the nematic-smectic A_1 ($N-A_1$) transition exhibited by materials whose constituent molecules do not have strongly polar end groups. We shall now discuss the results of our studies on materials with strongly polar cyano end group exhibiting $N-A_1$ (polar) transition. Although the molecular picture of A_1 phase (see Fig.3.1) does not show a difference between polar A_1 and non-polar A_1 phases, the dipoles being randomly distributed within the layer in the case of former, it is of interest to see if there is any difference in the dielectric behaviour between polar A_1 and non-polar A_1 systems. The materials studied by us are 4th, 6th and 8th members of the homologous series 4-(4'-alkoxybenzoyloxy)-4'-cyanoazobenzenes (nOBCAB).^{22,23} The transition temperatures for these materials have already been given (see Table 3.1).

3.5.1 Xray Results

Since no Xray data seem to be available on the layer spacing (d) in the A phases of these materials, we have measured the varia-

tion of d in the smectic A phase of all three substances. These data are given in Fig.3.9. It is seen that for all the materials, d is practically constant throughout A phase. It is also seen that d/ℓ value (where ℓ is the length of the molecule measured in its most extended configuration using Dreiding model) is about 0.94-0.95 for all the compounds. Therefore the A phase exhibited by these compounds is clearly the monolayer (A_1) phase. Differential scanning calorimetry (DSC) runs showed that the A-N transition is second order for all the three compounds.⁴⁰

3.5.2 Dielectric Results

a) Static

The static dielectric constants for 4OBCAB, 6OBCAB and 8OBCAB near the A_1 -N transition are shown in Figs. 3.10-3.12. We did not take any data near the nematic-isotropic (N-I) transitions since these temperatures are very high and the materials decomposed at these high temperatures. The main feature of the results on static dielectric constants is that for 4OBCAB a sharp drop in ϵ_{\parallel} is observed at N- A_1 transition. The value dropped from about 20 in nematic phase to about 14 in A phase. On the other hand the value of ϵ_{\perp} is practically unchanged through the N- A_1 transition. In the case of 6OBCAB (Fig. 3.11), a much smaller change in ϵ_{\parallel} is observed at the N- A_1 transition. This change is about

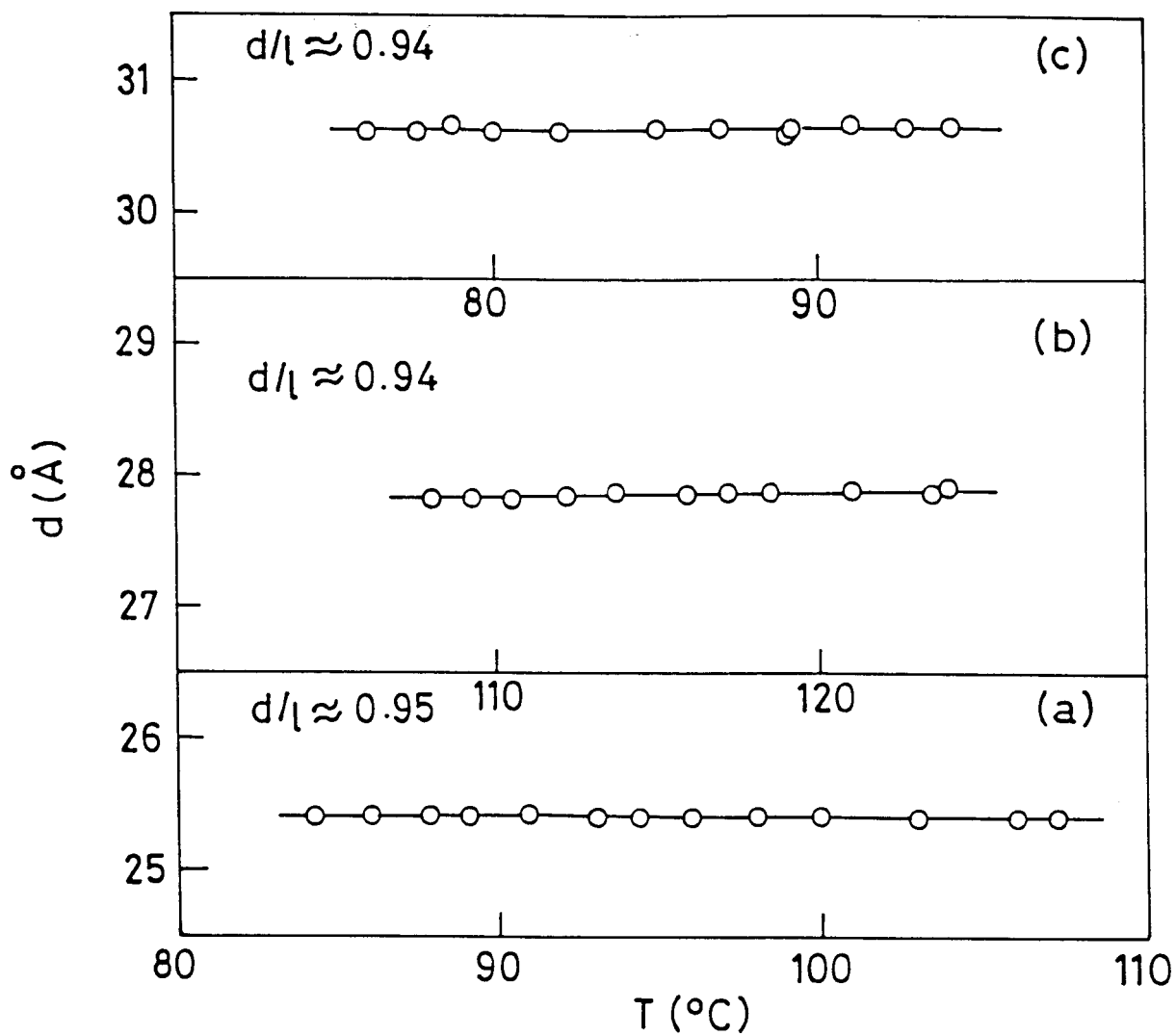


Figure 3.9

The temperature variation of the layer spacing (d) in the smectic A_1 phase of (a) 40BCAB, (b) 60BCAE and (c) 80BCAB.

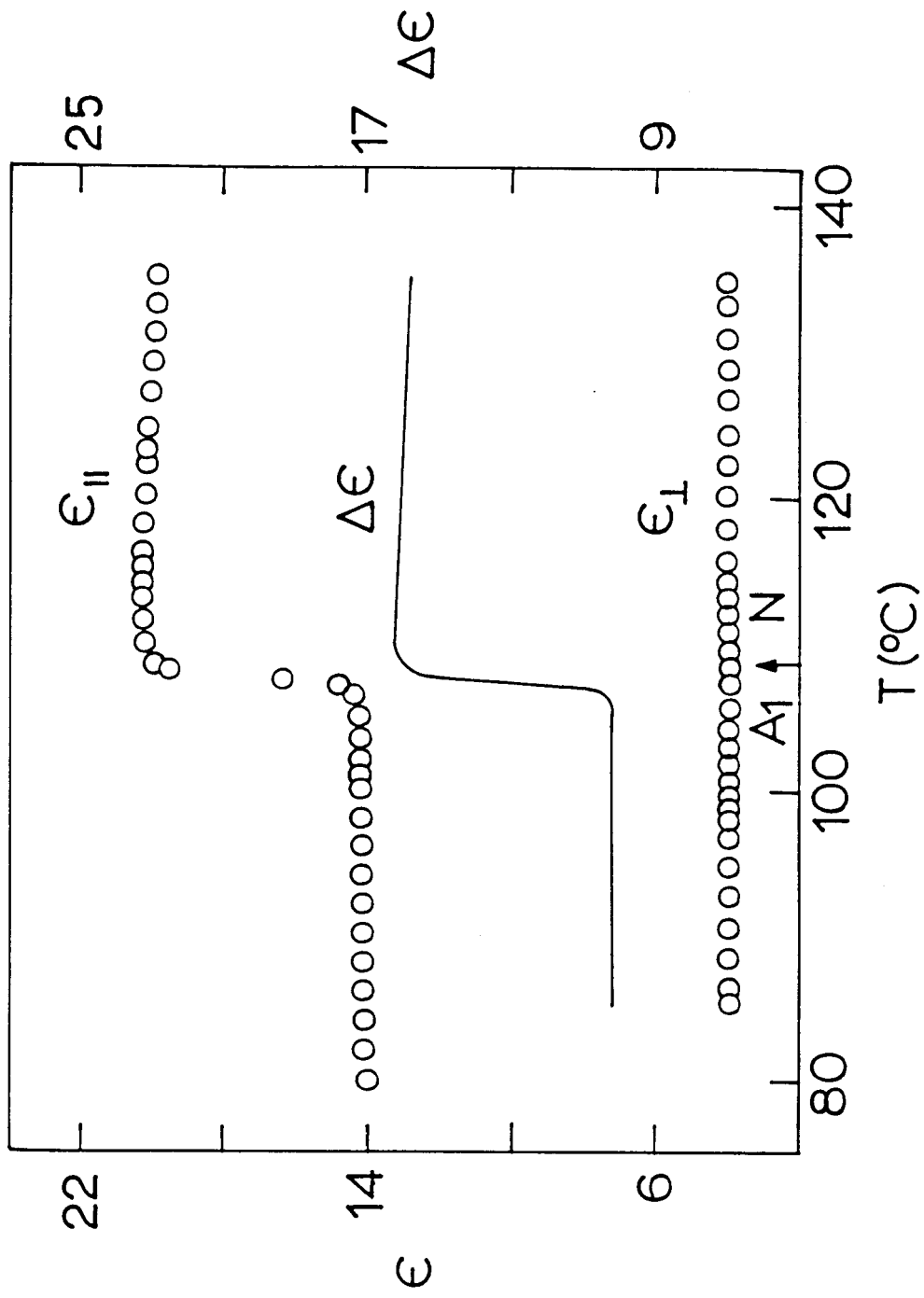


Figure 3.10: Temperature variation of the dielectric constants $\epsilon_{||}$ and ϵ_{\perp} and the dielectric anisotropy $\Delta\epsilon$ near the A_1-N transition of 4OBCAB.

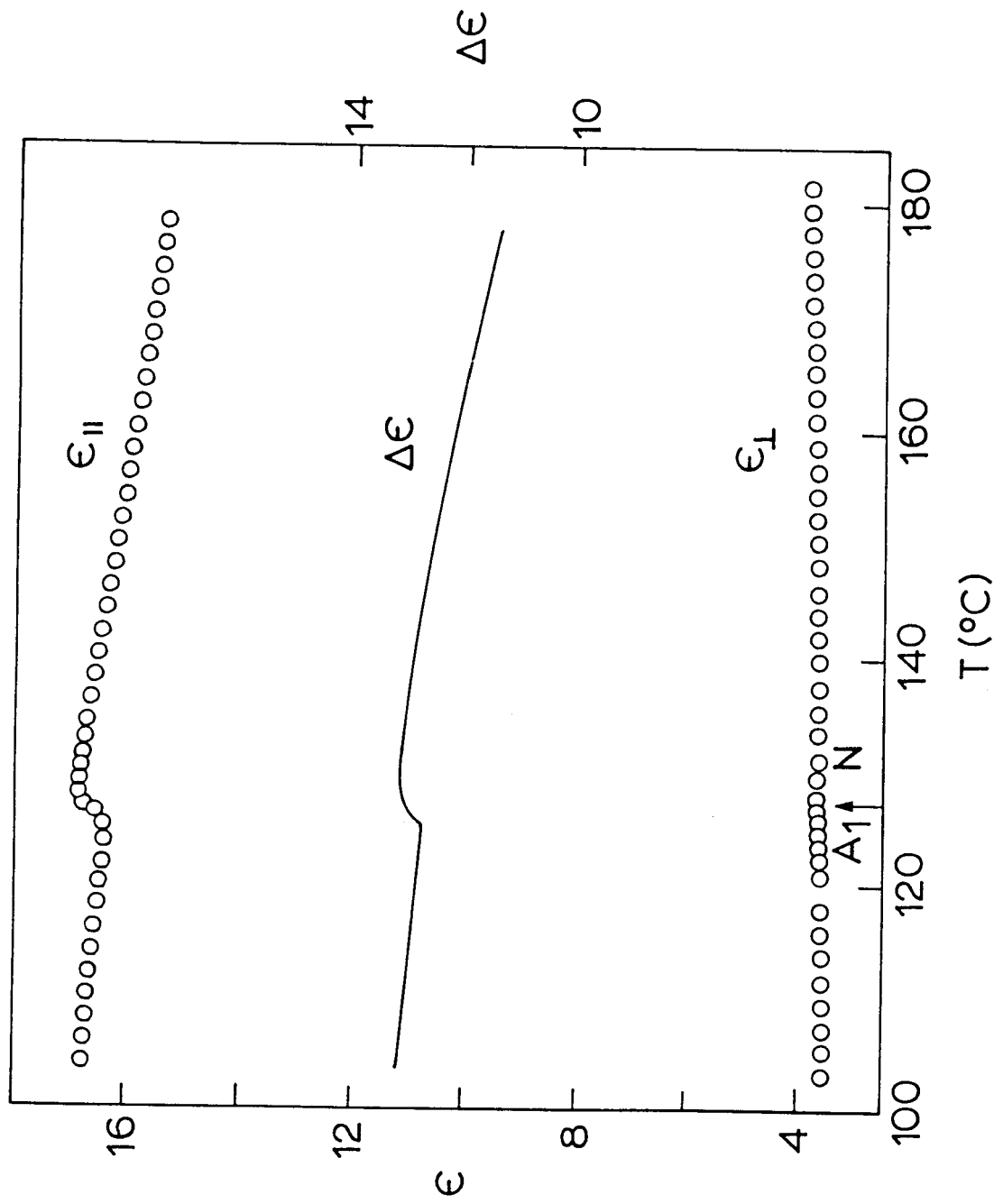


Figure 3.11: The temperature variation of ϵ_{\parallel} , ϵ_{\perp} and $\Delta\epsilon$ near A_1 - N transition of 60BCAB

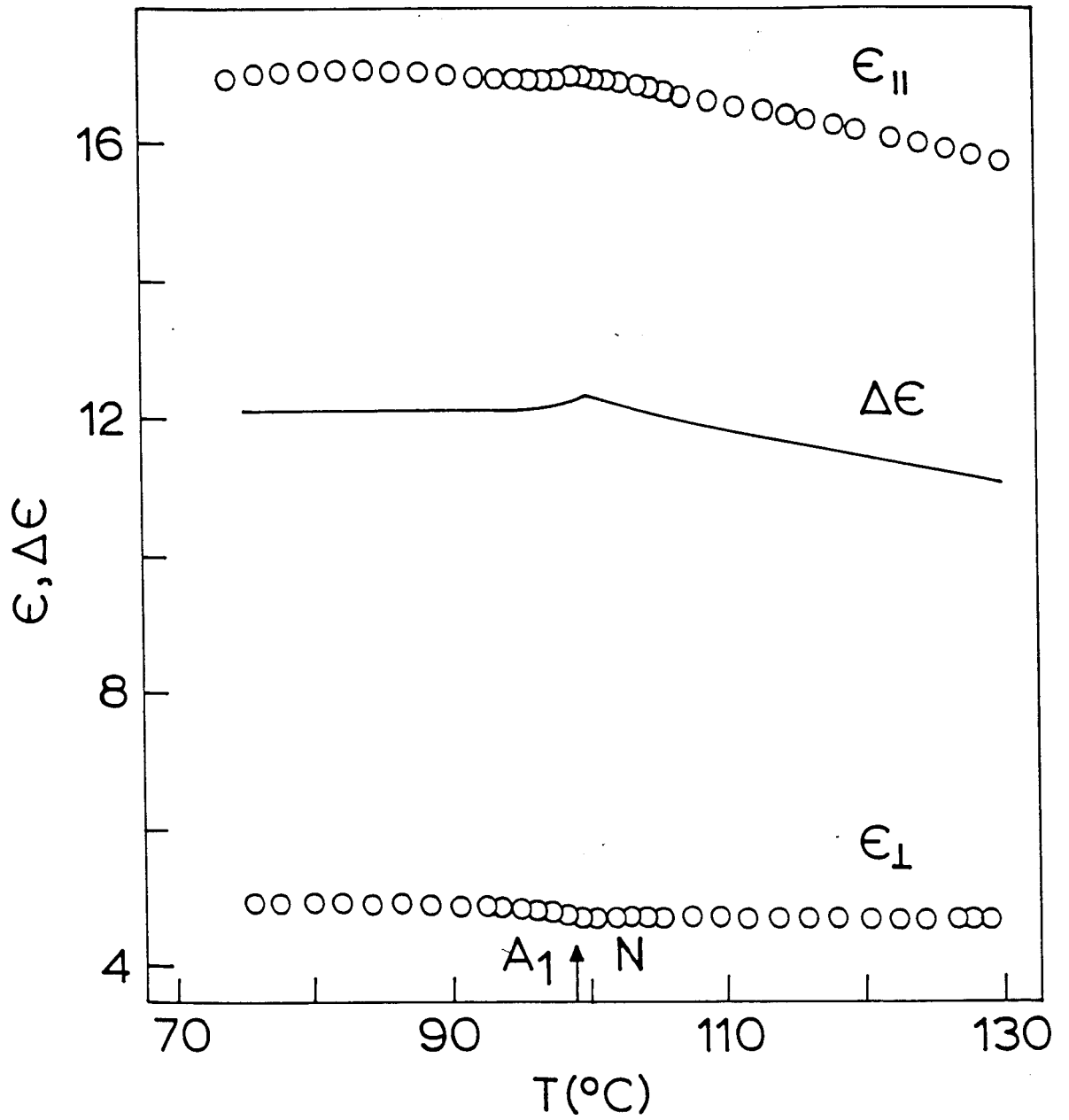


Figure 3.12

Temperature variation of $\epsilon_{||}$, ϵ_{\perp} and $\Delta\epsilon$ near the A₁-N transition of 80BCAB.

0.6 compared to 6 in the case of 4OBCAB. Also the change in ϵ_{\parallel} at A_1 -N transition in case of 6OBCAB is less sharp. Finally, for 8OBCAB, the change in ϵ_{\parallel} is hardly perceptible and only a change in slope is seen. These results seem to indicate that for 4OBCAB the antiparallel correlations in N and A_1 phases are substantially different whereas for 8OBCAB these correlations should be similar in the two phases. It is relevant to recall here the Xray studies of Hopf⁴¹ on 8OBCAB and 4OBCAB which showed significant differences in the local smectic-like ordering in the nematic phases of the two materials. This difference obviously manifests in a remarkable manner as a difference in the dielectric behaviour near the N-A transitions of these systems.

b Dispersion

Figures 3.13-3.15 show plots of dielectric loss (ϵ_{\parallel}'' vs. frequency) for 4OBCAB, 6OBCAB and 8OBCAB respectively. It is clear in all the cases that loss curves have clear maxima with symmetrical distribution of frequencies on either side of the frequency of relaxation. Typical Cole-Cole plots in N and A phases of the three materials are given in Figs.3.16-3.21. In all cases the Cole-Cole plots are seen to be perfect semicircles showing that there is a single relaxation process. The frequencies of relaxation f_R determined from loss curves and Cole-Cole plots for the three materials are shown in Tables 3.4-3.6. It is seen that f_R

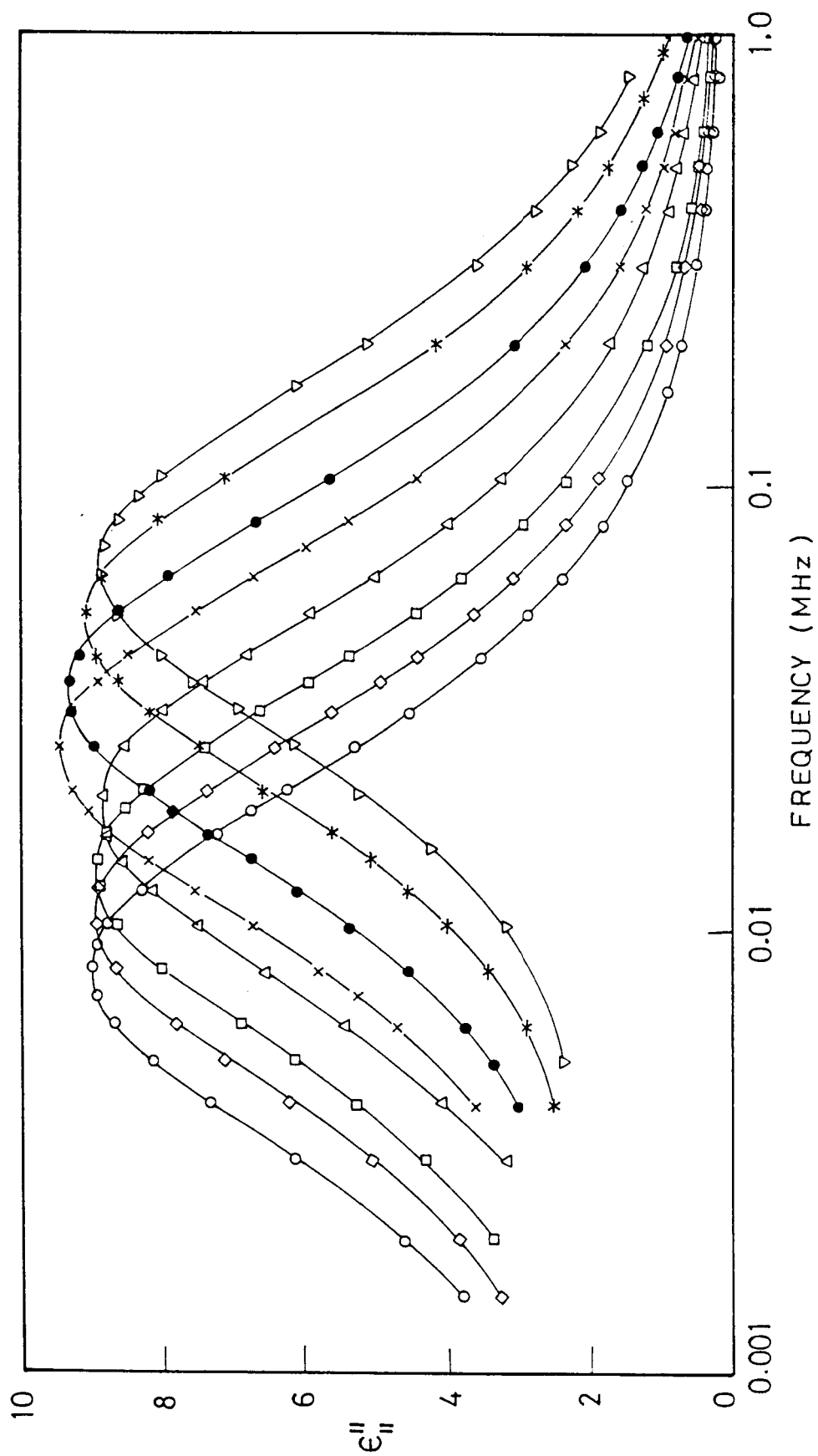


Figure 3.13: Representative loss curves of 4OBCAB in the (a) nematic (∇ 130.5°C, $*$ 125°C, \bullet 117.8°C, \times 111.5°C) and (b) smectic A_1 phase (Δ 105°C, \square 98.4°C, \diamond 94.2°C and \circ 89.4°C).

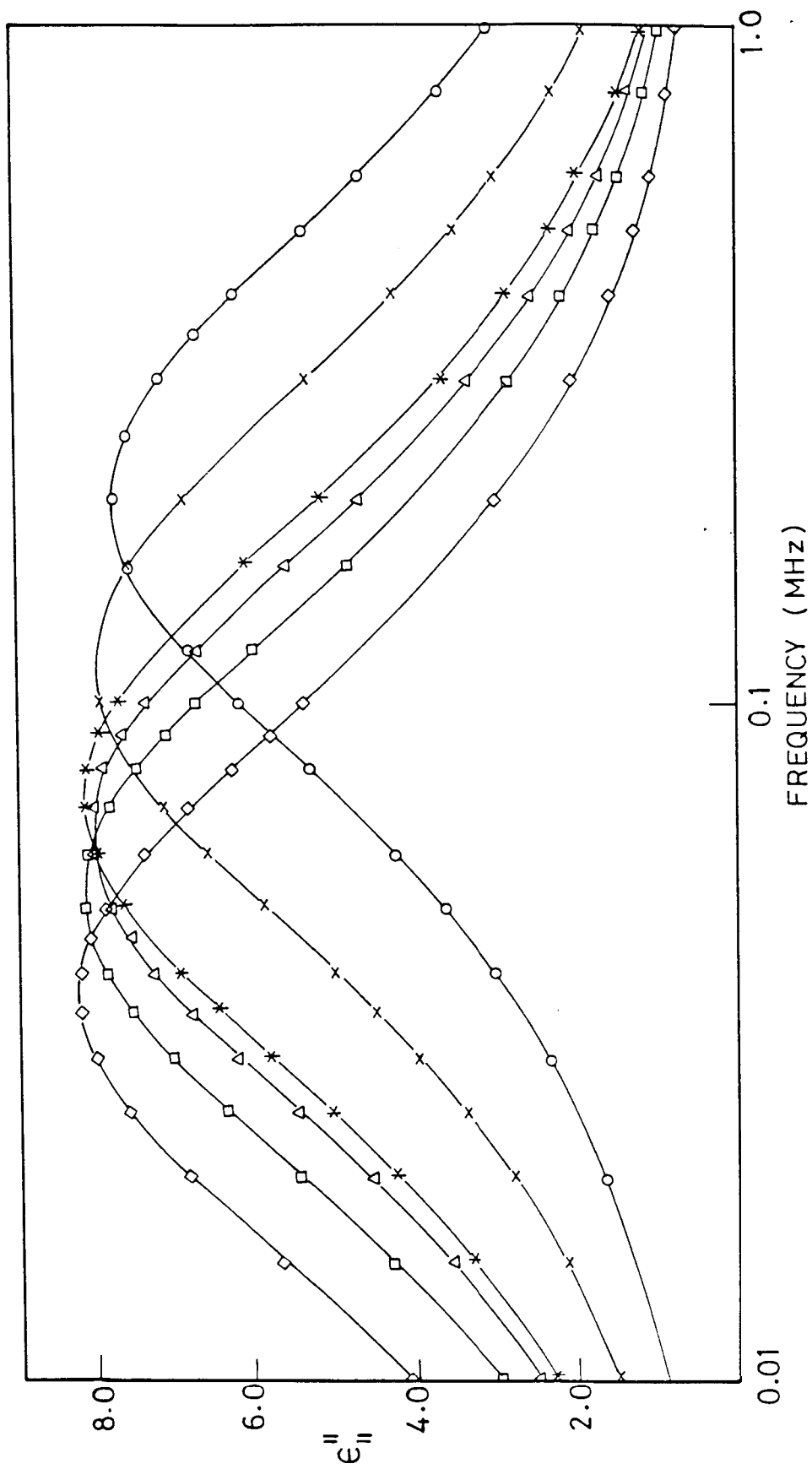


Figure 3.14. Representative loss curves of 60BCAB in the (a) nematic (○ 151°C, ✕ 138.1°C, * 128°C) and (b) smectic A_1 phase (◄ 125.6°C, ◻ 122°C and ◊ 115.8°C).

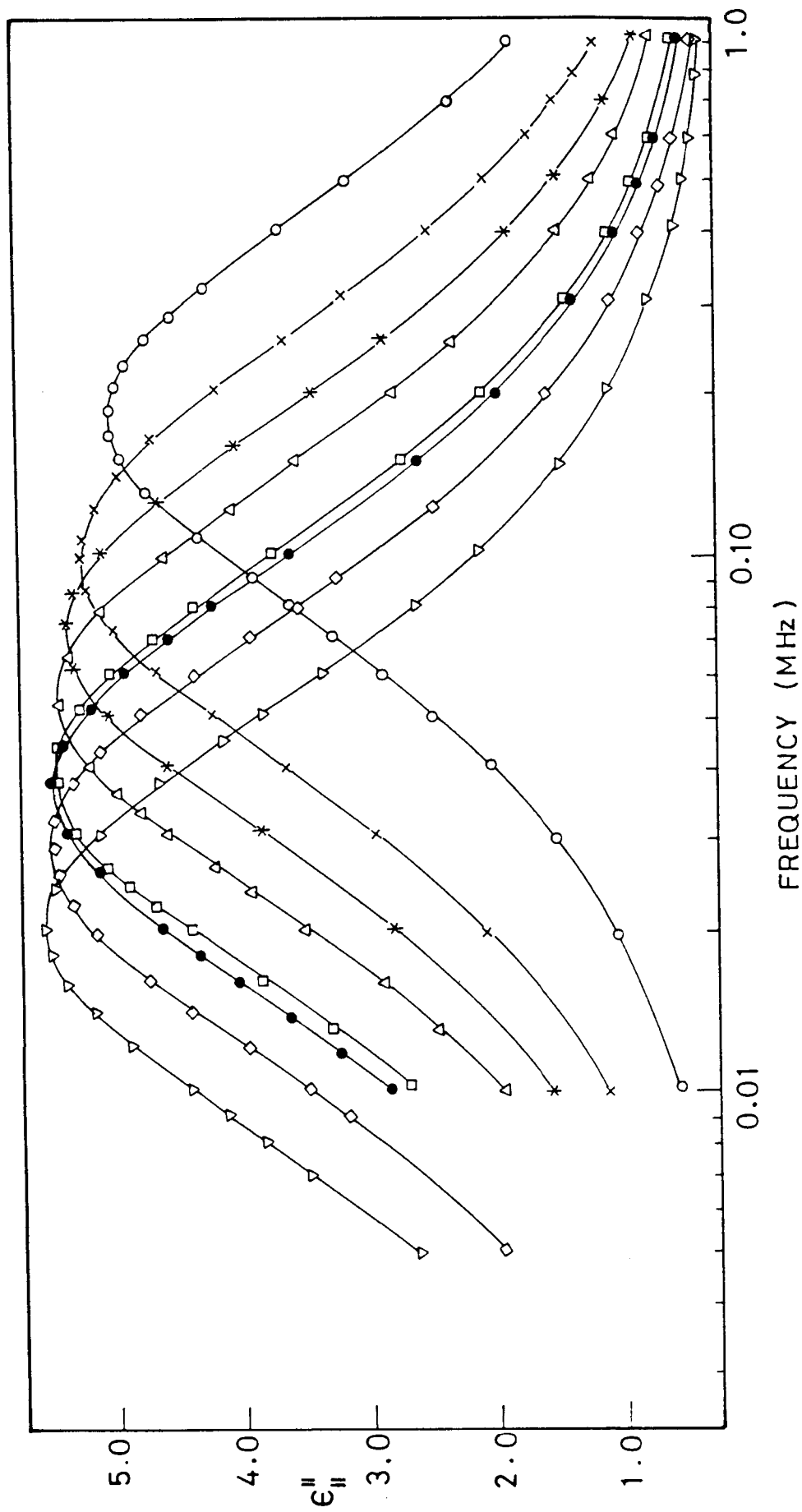


Figure 3.15. Representative loss curves of 80BCAB in the nematic (○ 121.5°C, × 111.8°C, * 106.5°C, Δ 102.8°C) and smectic A₁ phase (□ 98°C, ● 97.4°C, ◇ 93.7°C and ▽ 89.2°C)

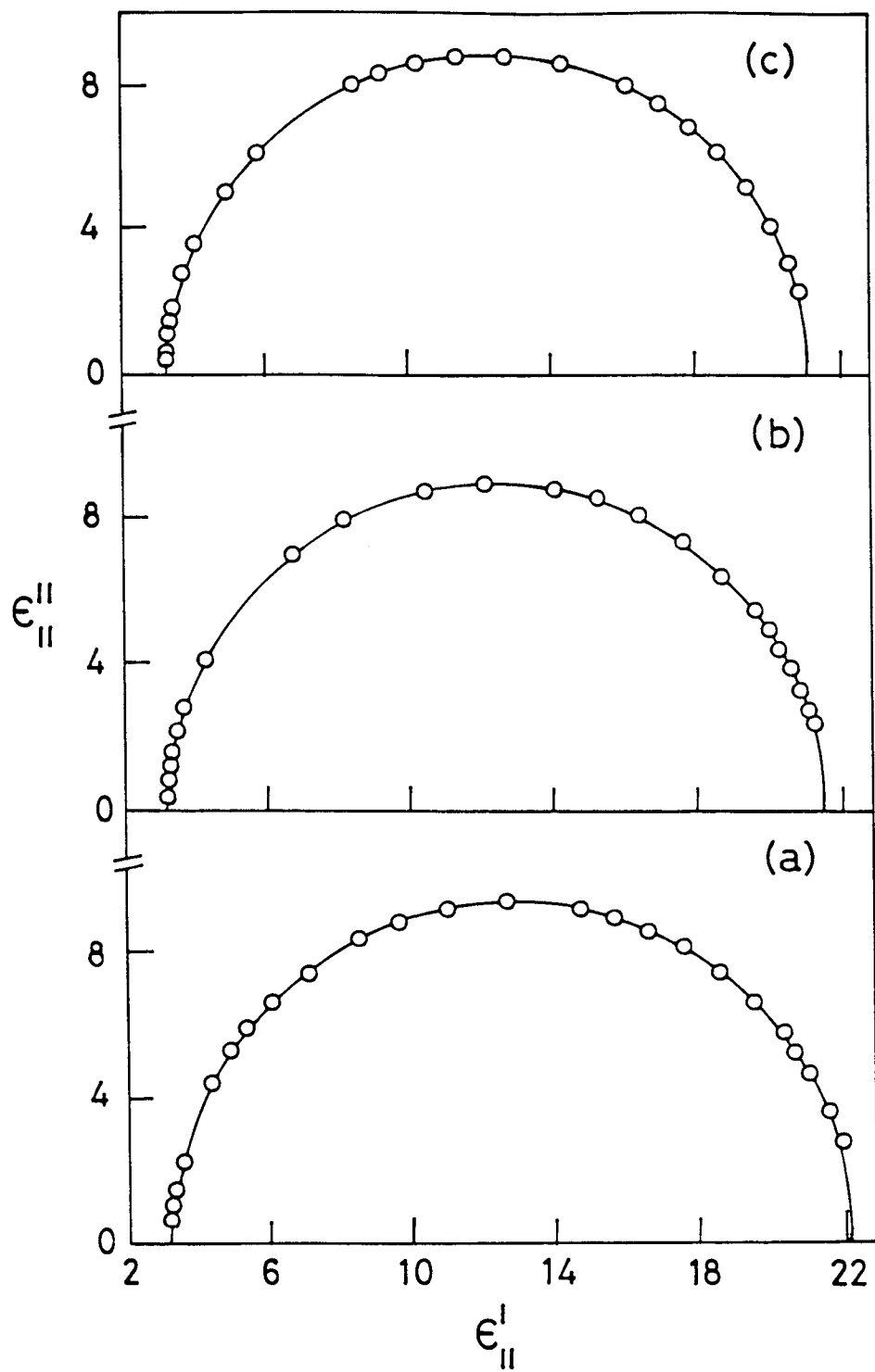


Figure 3.16

Representative Cole-Cole plots of 4OBCAB in the nematic phase at (a) 111.5°C (b) 125.0°C and (c) 130.5°C.

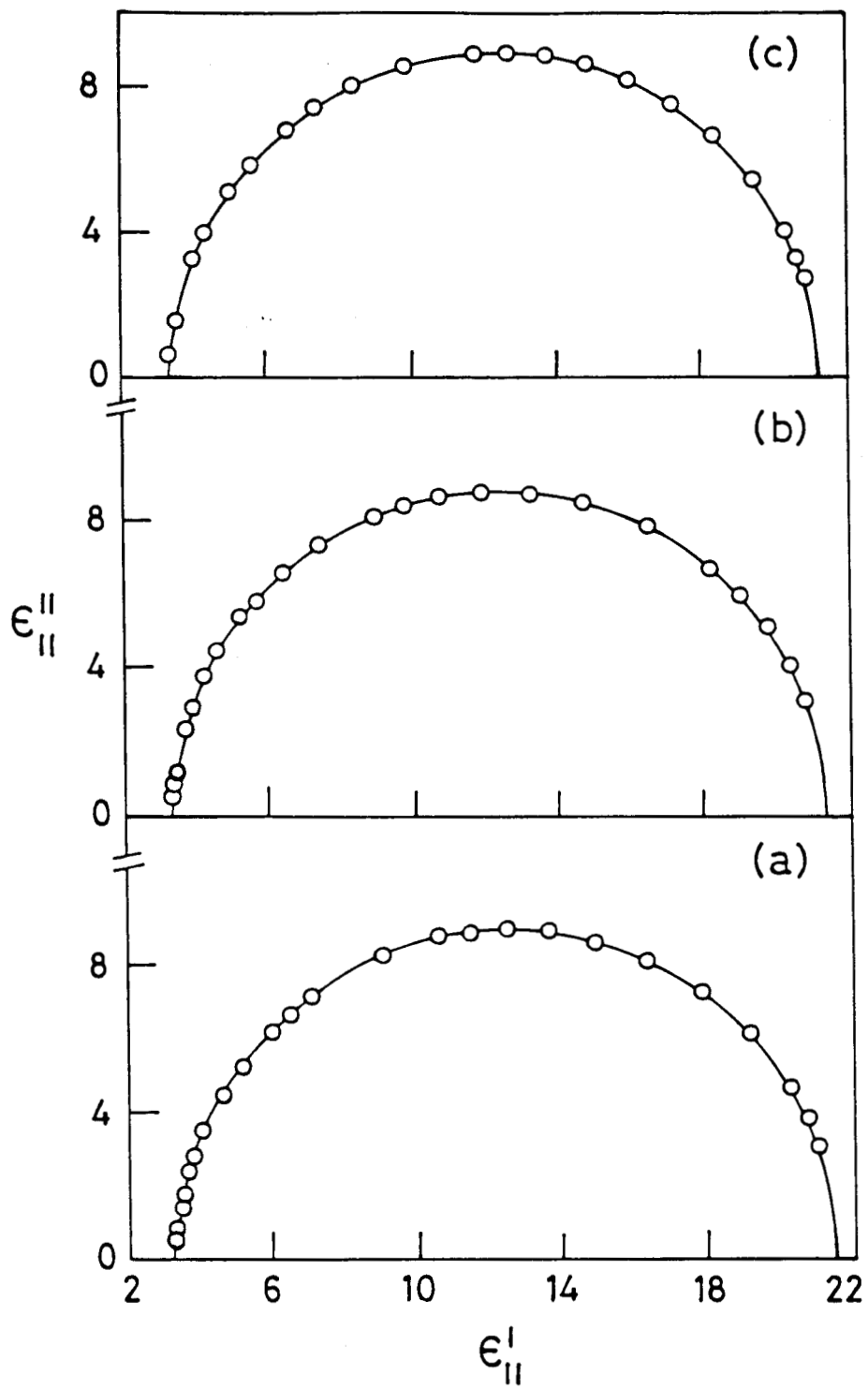


Figure 3.17

Representative Cole-Cole plots of 4OBCAB in the smectic A_1 phase at (a) 89.4°C, (b) 98.4°C and (c) 105.0°C.

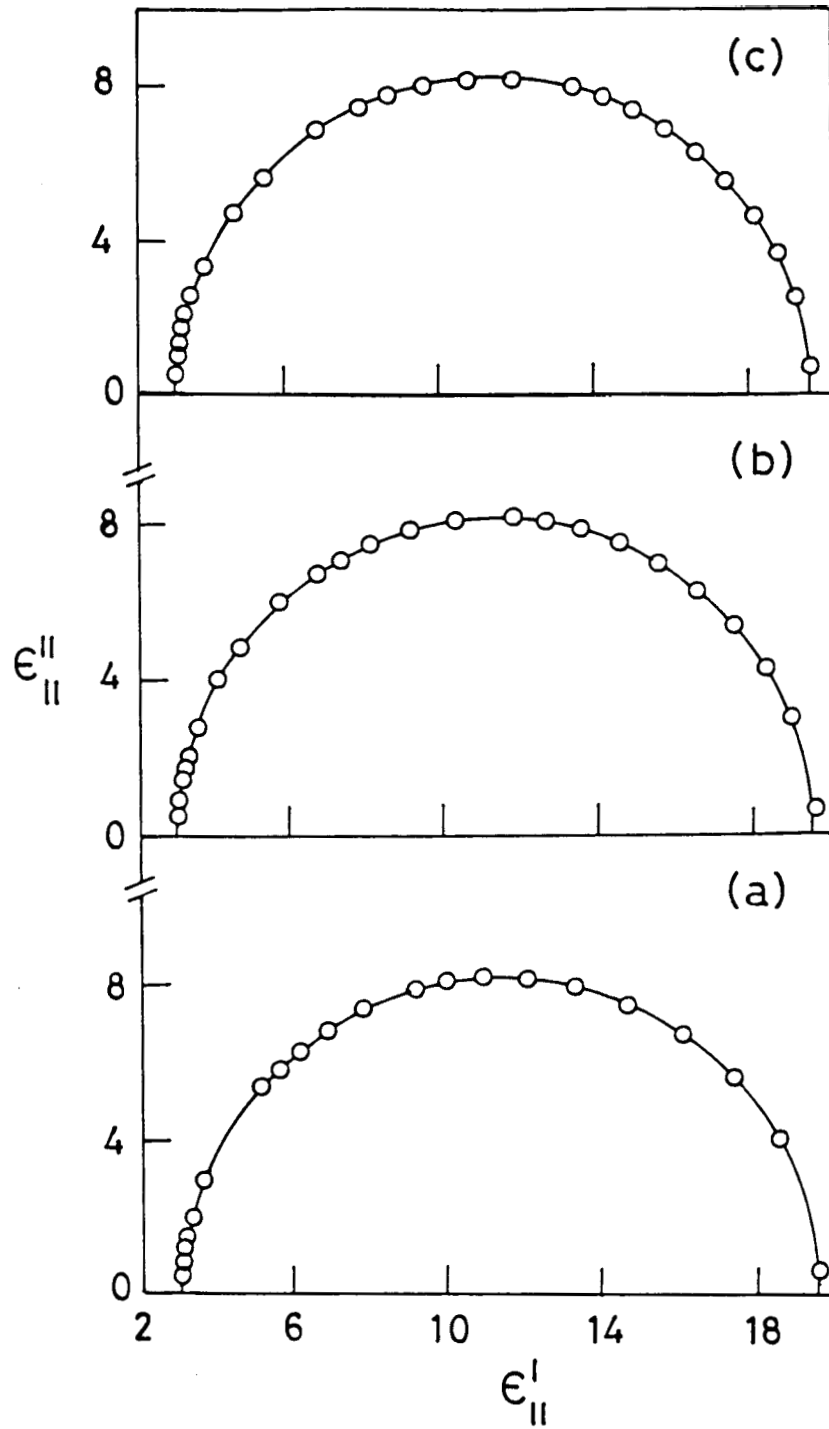


Figure 3.18

Representative Cole-Cole plots of 60BCAB in the nematic phase at (a) 128°C, (b) 138.1°C and (c) 151°C.

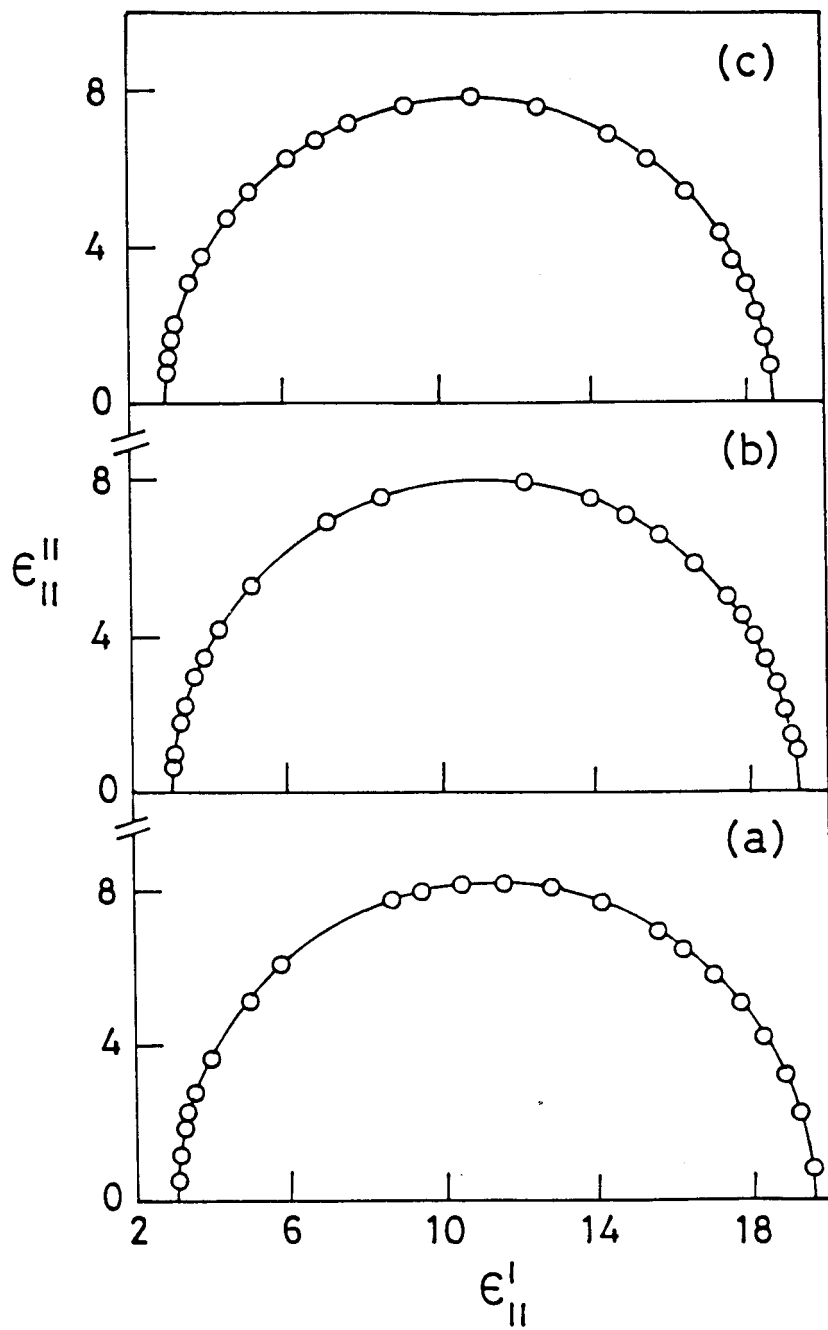


Figure 3.19

Representative Cole-Cole plots of 60BCAB in the smectic A1 phase at (a) 115.8°C, (b) 122°C and (c) 125.6°C.

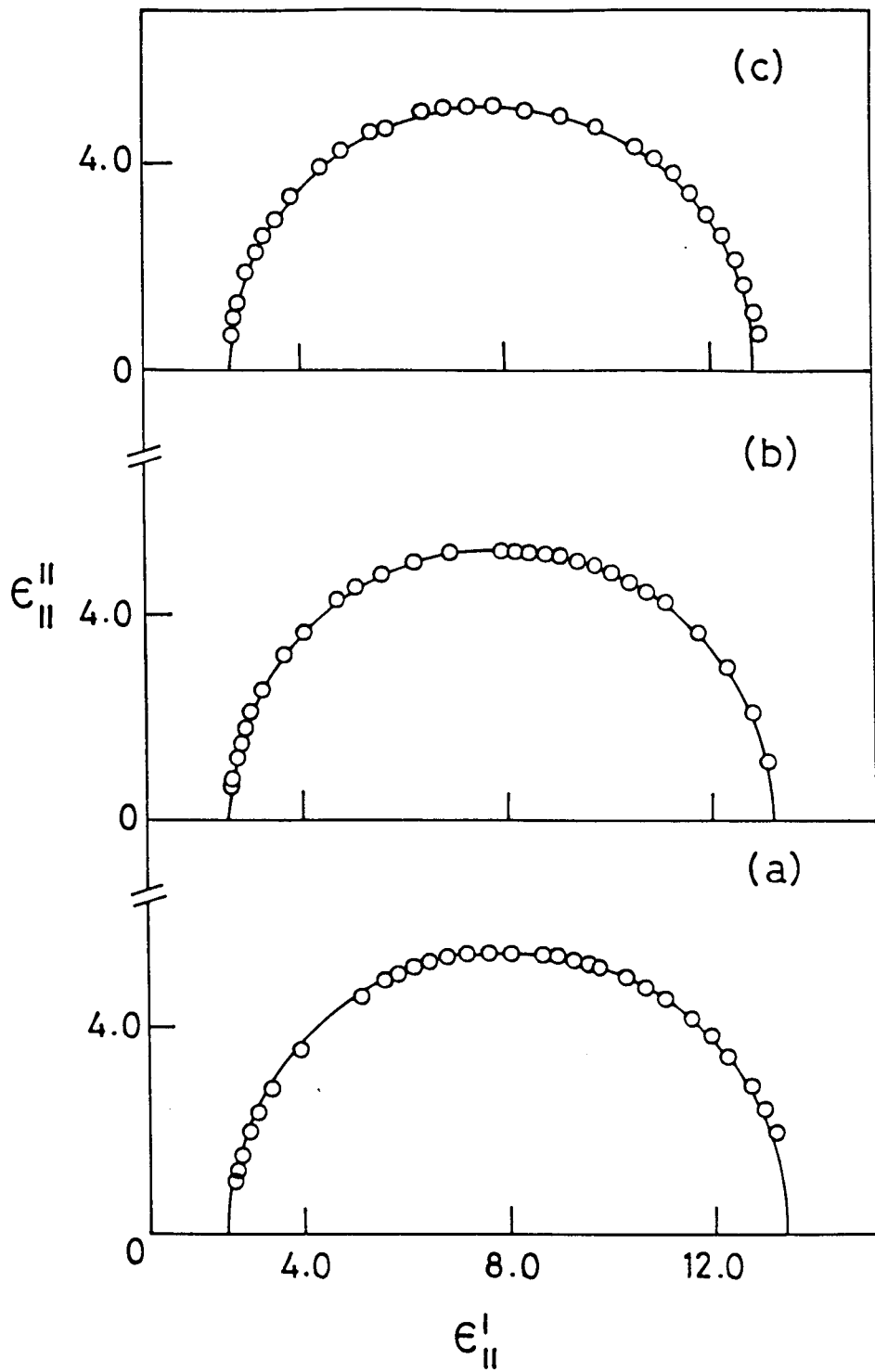


Figure 3.20

Representative Cole-Cole plots of 80BCAB in the nematic phase at (a) 102.8°C, (b) 111.8°C and (c) 121.5°C.

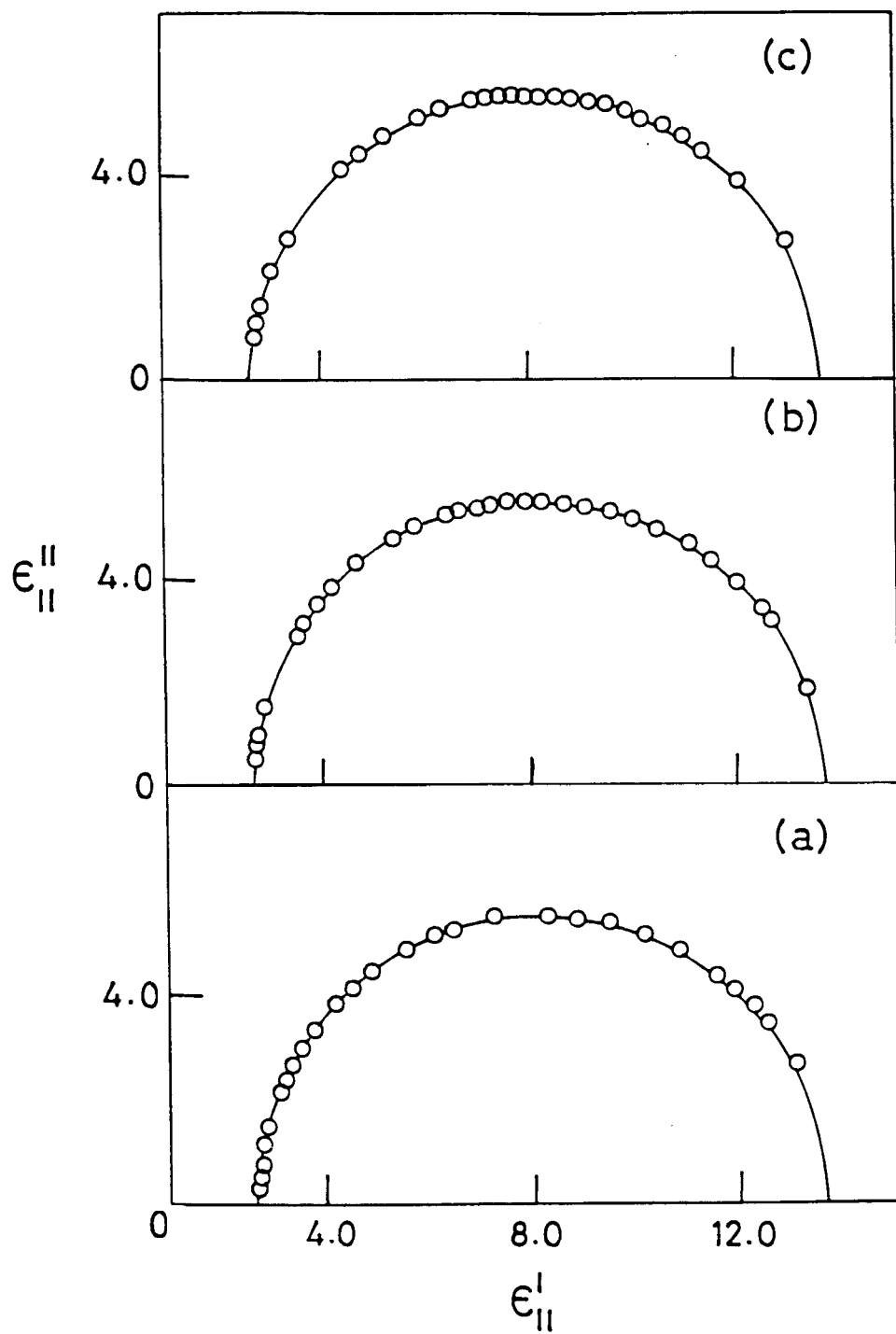


Figure 3.21

Representative Cole-Cole plots of 80BCAB in the smectic A, phase at (a) 89.2°C, (b) 93.7°C and (c) 98°C.

TABLE 34

Frequency of Relaxation (f_R) as a function of temperature in
nematic and smectic A_I phases of 4OBCAB

S.No.	Temperature (°C)	Frequency of Relaxation (in KHz)		Mean f_R
		From loss curve	From Cole-Cole	
<u>N Phase</u>				
1	130.5	64	63.47	63.74
2	124.95	48	48.34	48.17
3	121.15	40	40.31	40.16
4	117.8	34	33.69	33.85
5	114.4	28.5	28.67	28.59
6	111.5	24.75	24.62	24.69
7	110.25	24.0	24.3	24.15
<u>A_I Phase</u>				
8	107.25	20.05	21.14	20.60
9	105	18.6	18.73	18.67
10	102.35	16.1	16.03	16.07
11	98.35	13.0	13.1	13.05
12	94.15	10.4	10.52	10.46

TABLE 3.5

Frequency of relaxation (f_R) as a function of temperature in
nematic and smectic A_1 phases of 6OBCAB

S.No.	Temperature (°C)	Frequency of relaxation (in KHz)		Mean f_R
		From loss curve	From Cole-Cole	
<u>N P h a s e</u>				
1	154.2	230	229.41	229.71
2	151.0	202.5	204.6	203.55
3	146.6	167.5	169.0	168.25
4	141.2	132.0	134.2	133.10
5	138.1	115	115.16	115.08
6	134.6	98	97.43	97.72
7	130.9	82	82.27	82.14
8	128.0	72	71.71	71.86
<u>A₁ P h a s e</u>				
9	126.7	68	67.7	67.85
10	126.0	66	66.16	66.08
11	124.8	61.5	61.3	61.40
12	123.1	57	57.17	57.09
13	121.1	52	52.21	52.11
14	119.1	46	46.05	46.03
15	116.6	40.5	41.02	40.76

TABLE 3.6

Frequency of relaxation (f_R) as a function of temperature in
nematic and smectic A_1 phases of 8OBCAB

S. No.	Temperature (°C)	Frequency of relaxation (in KHz)		Mean f_R
		From loss curve	From Cole-Cole	
<u>N P h a s e</u>				
1	121.5	180	180	180
2	116.7	137	135	136
3	113.1	110	110	110
4	111.8	99	100	99.5
5	108.7	84	84	84
6	106.5	72	70	71
7	104.9	62.5	62.5	62.5
8	102.80	56	55	55.5
9	100.9	48	48	48
10	100	45	45	45
<u>A₁ P h a s e</u>				
11	98.7	41	42	41.5
12	98.0	40	39	39.5
13	97.4	37	37	37
14	93.7	29	28	28.5
15	89.2	21	20	20.5

determined from these are nearly the same. The plots of f_R versus $1/T$ in N and A phases of the three materials are shown in Figure 3.22. The activation energies (W) calculated from the slopes of these plots are also shown in Fig.3.22. It is clear that $W_N > W_A$ in the case of 4OBCAB while $W_N < W_A$ in the case of both 6OBCAB and 8OBCAB. This difference could well be due to the differences in the cybotactic smectic ordering in the nematic phases of the materials as discussed earlier. However due to the uncertainties in the determination of W , no definite conclusions can be reached.

3.6 NEMATIC-SMECTIC A_d TRANSITION

In this section, we present our results on dielectric measurements near the nematic-smectic A_d ($N-A_d$) transition in 4-cyano-benzylidene-4'-n-octyloxyaniline (CBOOA). Since the transition temperatures of this material (see Table 3.1) are low, it is possible to make measurements in isotropic, nematic and smectic A_d phases.

3.6.1. Static Permittivities

The variation of static dielectric constants with temperature is shown in Fig.3.23. As mentioned earlier, the A_d -N transition of CBOOA has been studied by a variety of techniques.³¹ In particular, high resolution Xray studies³³ clearly showed that this transition is second order. The variation of ϵ_{\parallel} near $N-A_d$ transition is typical of what has been seen in other similar substances, e.g.,

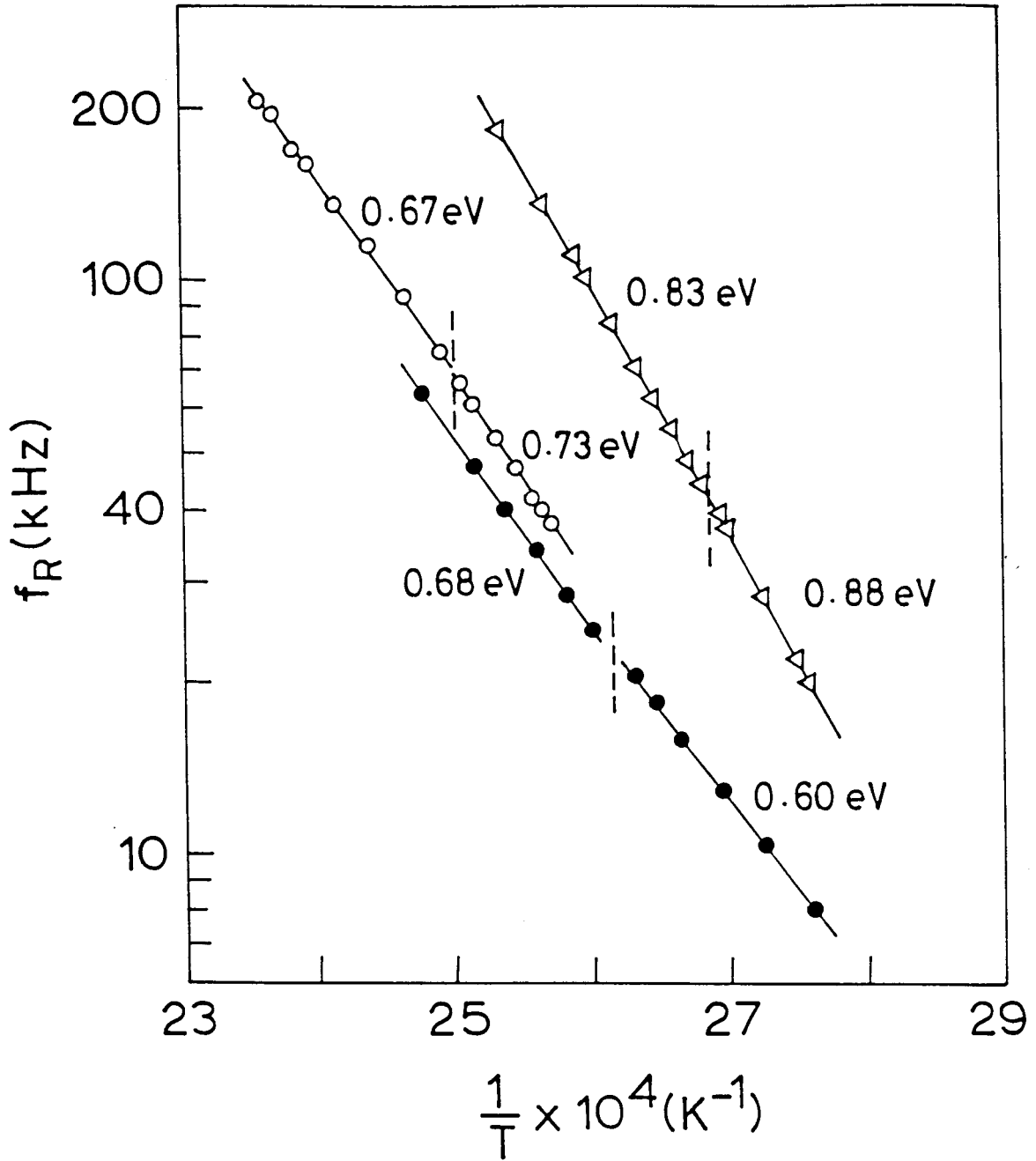


Figure 3.22

Plot of the relaxation frequency f_R versus $1/T$; ● 40BCAB, ○ 60BCAB and △ 80BCAB. The vertical dashed line indicates the A_1-N transition temperature. The activation energies are also given.

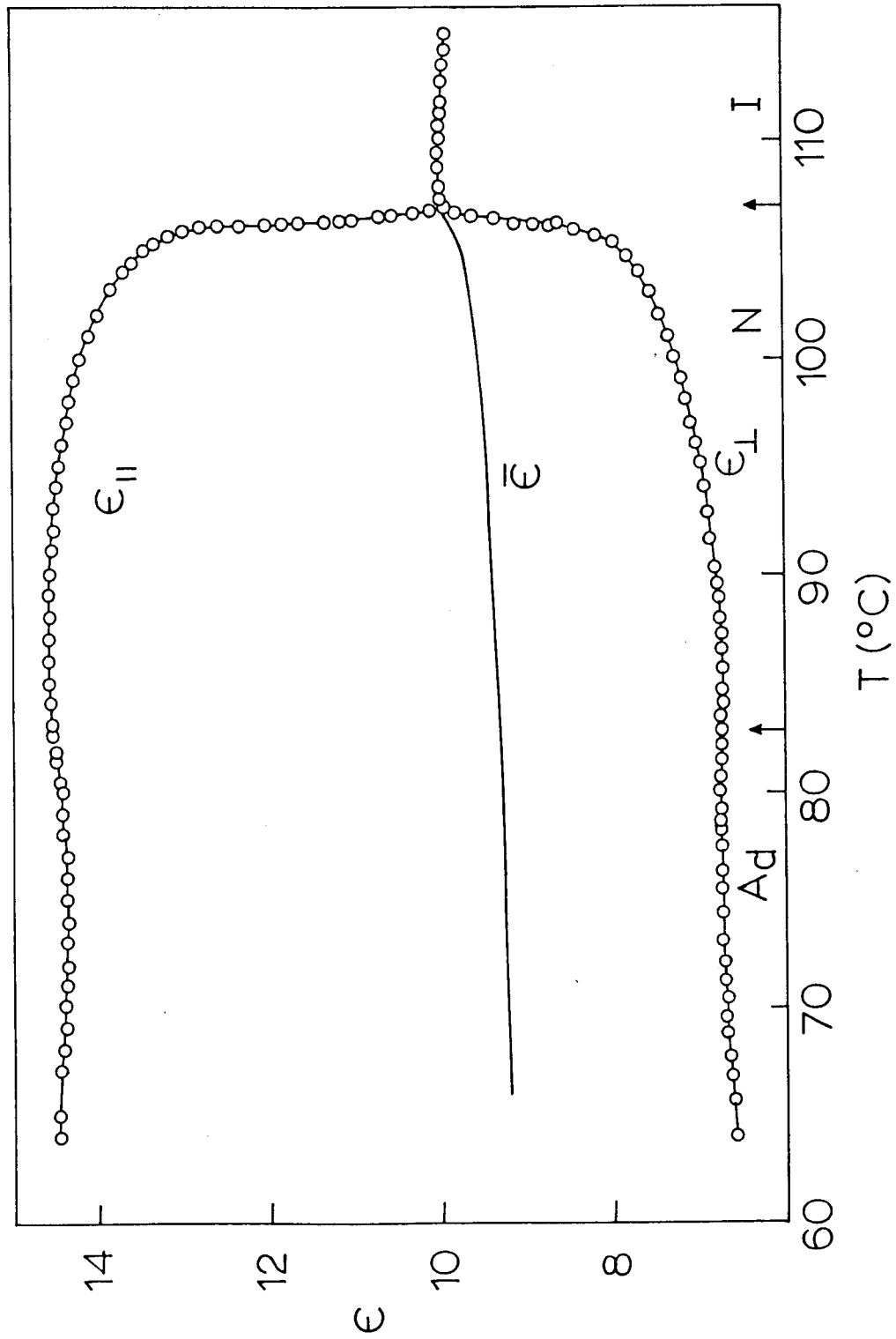


Figure 3.23. Temperature variation of the dielectric constants $\epsilon_{||}$, ϵ_{\perp} and of the mean dielectric constant $\bar{\epsilon}$ of CB00A.

4'-n-octyl-4-cyanobiphenyl (8CB),^{15,17,30,42,43} 4'-n-octyloxy-4-cyanobiphenyl (8OCB),^{21,43} etc. — there is only a very small decrease in ϵ_{\parallel} at the N-A transition, ϵ_{\parallel} getting saturated in the A_d phase. It is also seen that the average dielectric constant ($\bar{\epsilon}$), calculated from the experimentally determined values of ϵ_{\parallel} and ϵ_{\perp} using the relation $\bar{\epsilon} = (\epsilon_{\parallel} + 2\epsilon_{\perp})/3$, is less than the extrapolated isotropic value (ϵ_{is}) throughout the N and A phases. It may be recalled that Madhusudana and Chandrasekhar⁵ theoretically postulated that the signature of near neighbour antiparallel correlations in materials with a strongly polar end groups should be seen in dielectric properties— $\bar{\epsilon}$ should be less than ϵ_{is} owing to increased antiparallel correlations on going from isotropic to nematic phase. This prediction has in fact been verified in a number of materials. In CBOOA also such a behaviour is seen as expected.

3.6.2. Dispersion

The loss curves i.e., ϵ''_{\parallel} versus frequency plots for some typical temperatures in N and A_d phases of CBOOA are shown in Fig.3.24 while typical Cole-Cole plots are shown in Fig.3.25. It is clear from these plots that the relaxation process is well defined, there being only one relaxation. The values of f_R obtained are shown in Table 3.7. The Arrhenius plot of f_R versus $1/T$ is shown in Fig.3.26. The feature of the figure is that the activation

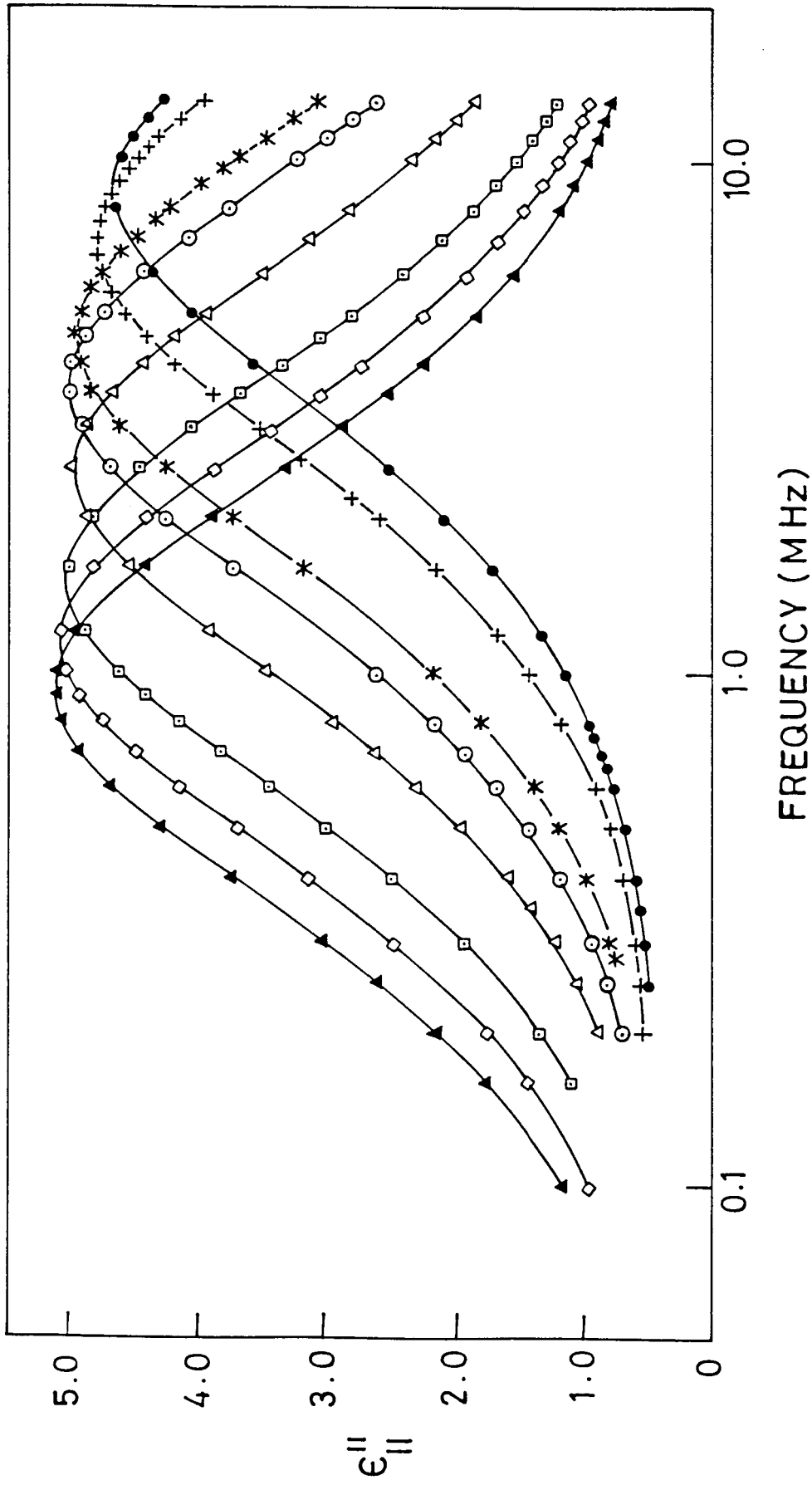


Figure 3.24. Representative loss curves of CB00A in the nematic (● 100.1°C, + 95.8°C, * 88.1°C, ○ 84°C) and smectic A_d (△ 76.3°C, □ 67.4°C, ◇ 63.1°C and ▲ 59.3°C) phases.

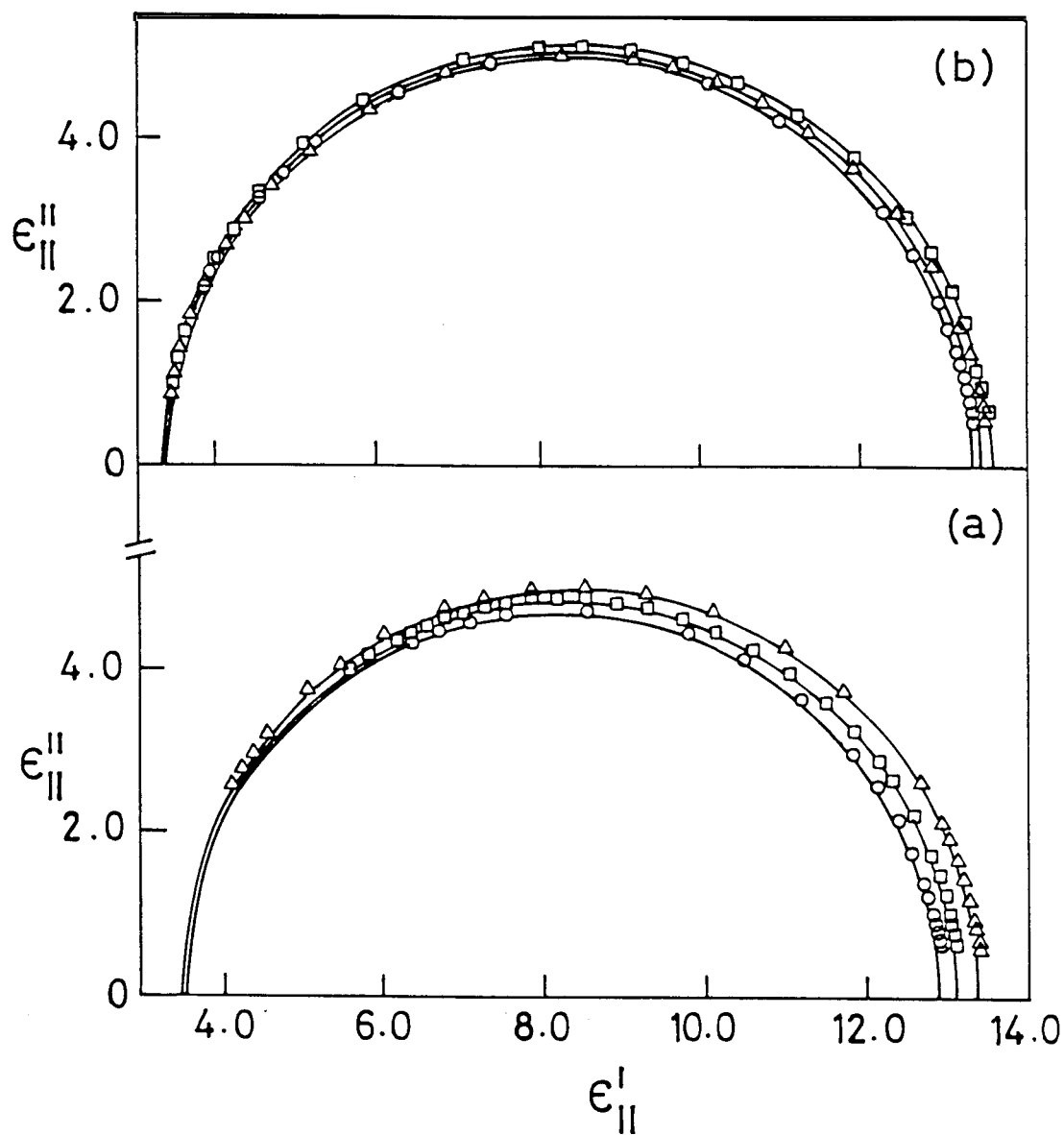


Figure 3.25

Representative Cole-Cole plots of CBOOA in the (a) nematic (o 100.1°C, □ 95.8°C, ▲ 84°C) and (b) smectic A_d (o 76.3°C, ▲ 63.1°C and □ 59.3°C) phases.

TABLE 3.7

Frequency of relaxation (f_R) as a function of temperature in
nematic and smectic A_d phases of CBOOA

S. No.	Temperature (°C)	Frequency of relaxation (in MHz)		Mean f_R
		From loss curve	From Cole-Cole	
<u>N e m a t i c</u>				
1	100.1	8.55	8.58	8.57
2	98.20	7.50	7.40	7.45
3	95.8	6.8	6.92	6.86
4	94.30	6.0	6.02	6.01
5	91.7	5.4	5.46	5.43
6	89.8	4.9	4.7	4.8
7	88.1	4.4	4.41	4.405
8	87.5	4.1	4.17	4.135
9	85.7	3.9	3.89	3.895
10	84.0	3.58	3.59	3.585
11	83.9	3.5	3.49	3.495
<u>S m e c t i c A_d</u>				
12	81.9	3.2	3.2	3.2
13	79.6	2.86	2.9	2.88
14	78.0	2.63	2.65	2.64
15	76.3	2.45	2.46	2.455
16	74.9	2.27	2.25	2.26
17	72.8	1.98	1.98	1.98
18	71.9	1.95	1.95	1.95
19	67.4	1.5	1.52	1.51
20	65.0	1.31	1.32	1.315
21	63.1	1.17	1.16	1.165
22	61.2	1.04	1.03	1.035
23	59.3	0.92	0.92	0.920
24	55.1	0.725	0.728	0.727

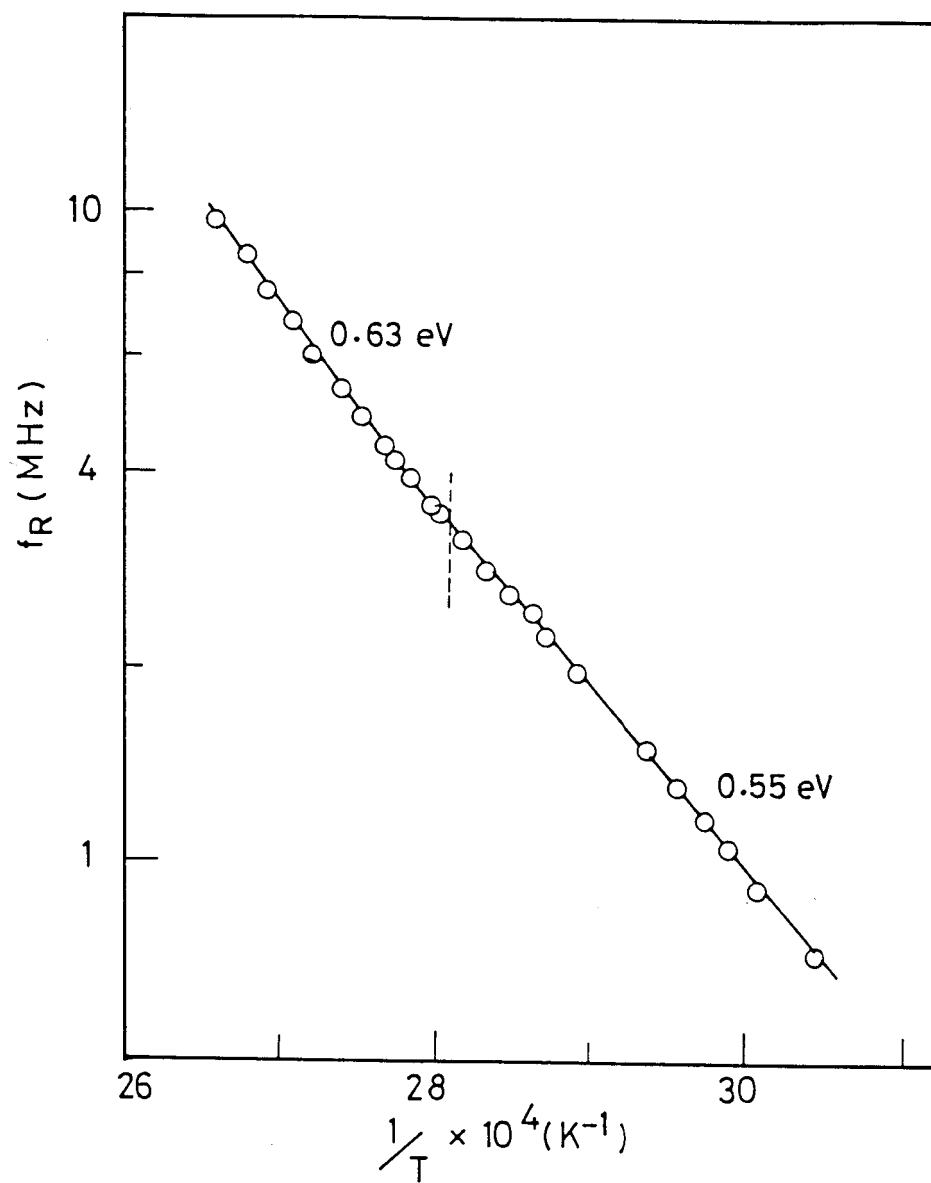


Figure 3.26

f_R versus $1/T$ plot of CBOOA. The dashed vertical line indicates $A_d - N$ transition. The activation energies are also shown.

energy in the A_d phase (W_{A_d}) is significantly lower than that of nematic (W_N). This behaviour, viz., $W_{A_d} < W_N$ has in fact been seen for most of the materials¹⁶⁻²⁰ showing the A_d phase.

3.7 NEMATIC-SMECTIC A_2 (N- A_2) TRANSITION

The transition between nematic and smectic A_2 phases is perhaps the least studied of all the nematic-smectic A (N-A) transitions. As remarked earlier this A_2 phase is a true bilayer phase with characteristic Xray diffraction maxima at $d=R$ and $d=2\ell$, where d is the layer spacing and ℓ is the length of the molecule in its most extended configuration. From their Xray measurements, Hardouin et al.¹⁰ concluded that A_2 phase is the result of a true long-range antiferroelectric ordering. This long range ordering in the direction of the long molecular axis is to be distinguished from the head-to-head near neighbour antiferroelectric ordering which is generally assumed to explain the dielectric properties of the A phases. Thus one would expect different dielectric properties at N- A_2 transition. The earlier studies of the N- A_2 transition are due to Benguigui and Hardouin⁴⁴ and to Druon et al.⁴⁵ on 4-n-hexylphenyl-4'-cyanobenzoyloxy benzoate (DB6CN) and also due to Benguigui et al.⁴⁶ on octyl-phenyl-2-chloro-4-(p-cyanobenzoyloxy)benzoate (DB₈Cl). We shall describe these results later. We have studied the N- A_2 transition in 4-n-pentylphenyl-4'-cyanobenzoyloxybenzoate (DB5CN).

3.7.1. Results and Discussion

a) Static

The variation of the static dielectric constants as well as the dielectric anisotropy ($\Delta\epsilon$) with temperature in the neighbourhood of the N- A_2 transition is shown in Fig.3.27. The important feature of these results is the strong decrease of ϵ_{\parallel} at the N- A_2 transition. This decreasing trend in ϵ_{\parallel} which continues throughout the A_2 phase can be attributed to the decrease in the effective longitudinal dipole moment due to head-to-head arrangement of the neighbouring dipoles accompanying the formation of the bilayer phase A_2 . ϵ_{\perp} shows only a small increase on going from nematic to A_2 phase indicating that the molecular rotation in A_2 phase is slightly hindered compared to that in N phase. It is recalled that Druon et al.⁴⁵ have seen almost exactly the same results on DB6CN. Benguigui and Hardouin⁴⁴ who have also studied DB6CN have observed a decrease in ϵ_{\parallel} as in our case but in addition they have seen the decrease of ϵ_{\perp} with decrease in temperature. This is in contrast to our observation on DB5CN and to that of Druon et al.⁴⁵ on DB6CN where ϵ_{\perp} was found to increase slightly on going from N to A_2 phase, while it remained constant in the A_2 phase.

Another feature of our results on DB5CN (see Fig.3.27) is the strong decrease in $\Delta\epsilon$ observed with decrease in temperature.

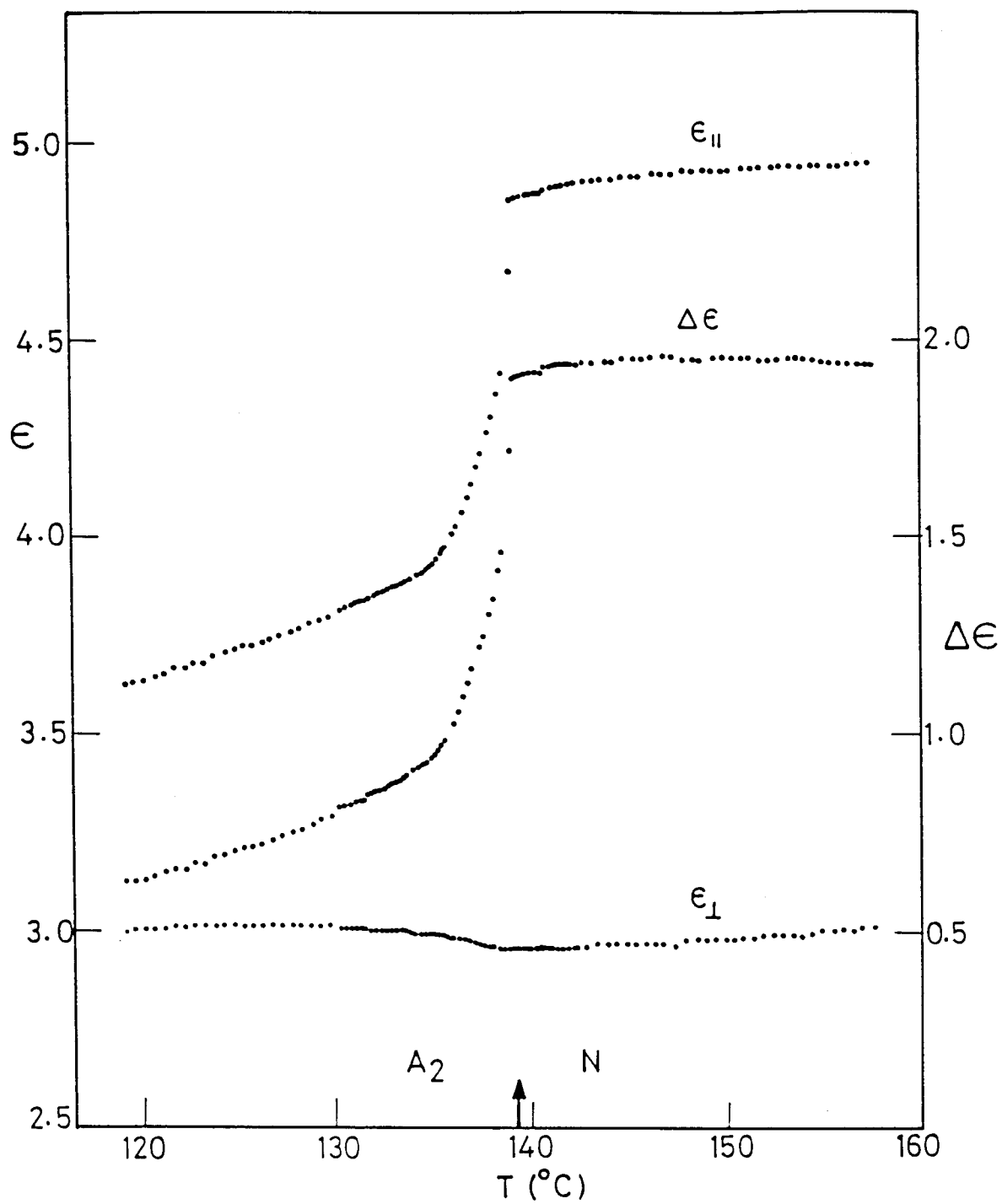


Figure 3.27

Temperature variation of dielectric constants $\epsilon_{||}$, ϵ_{\perp} and of $\Delta\epsilon$ in the nematic and smectic A_2 phases of DB5CN.

The dielectric anisotropy $\Delta\epsilon$ which is -2 in N phase drops suddenly at N- A_2 transition and decreases throughout A_2 phase attaining a value of -0.6 at the lowest temperature in A_2 phase. It is evident that if the material had been supercooled the $\Delta\epsilon$ would have conceivably changed sign. Such a reversal in the sign of $\Delta\epsilon$ is seen in the A_2 phase of DB_8Cl by Benguigui et al.⁴⁶

Thus it is clear from static dielectric constants that there is a strong head-to-head dipolar arrangement of molecules on formation of A_2 phase leading to a drastic reduction in ϵ_{\parallel} and hence $\Delta\epsilon$.

b) Dispersion

The dielectric dispersion study in the smectic A_2 phase has been the subject of some discussions of late. Benguigui in his theory⁷ of the Lifshitz point⁴⁸ in smectic A phases has discussed the dielectric behaviour in smectic A_1 , smectic A_2 and smectic \tilde{A} phases. He has predicted the existence of a single relaxation mode in polar A_1 phase, but two relaxation modes in the \tilde{A} and A_2 phases. The additional relaxation mode is expected to be related to a collective phenomenon similar to that seen in solid ferroelectric materials. The experimental results on dielectric dispersion of A_2 phase have been somewhat conflicting. Benguigui and Hardouin⁴⁴ reported observation of two relaxations for ϵ_{\parallel} in the A_2 phase

of 4-n-hexylphenyl-4'-cyanobenzoyloxy benzoate/terephthal-bis-4-n-butylaniline (DB6CN/TBBA) mixture as well as in pure DB6CN. Druon et al.,⁴⁵ from subsequent experiments on DB6CN seem to show clearly that A_2 phase of this material has only a single relaxation. This is in contrast to the result of Benguigui and Hardouin.⁴⁴ However it should also be mentioned that Druon et al.⁴⁵ did observe two superimposed relaxations in the A_2 phase of a binary mixture, viz., 4-n-hexylphenyl-4'-cyanobenzoyloxy benzoate/4-cyanobenzoyloxy-4'-pentyl stilbene (DB6CN/ C_5 Stilbene). They have argued⁴⁵ that the two dispersions seen in the A_2 phase of DB6CN/ C_5 stilbene mixture are probably due to the reorientations of the two molecular species. DB6CN molecule has two transverse dipole moments whereas C_5 stilbene has only one so that in the A_2 phase, the interactions of these molecules with the surroundings will be different, so much so, the reorientational motion of one of these can conceivably be easier than that of the other.

We present here the results of our dielectric studies in N and A_2 phases of DB5CN. The typical loss curves in N and A_2 phases are shown in Fig.3.28 while Cole-Cole plots for temperatures well inside N and A_2 phases are shown in Fig.3.29. These curves clearly show a single relaxation process in both N and A_2 phases. An interesting feature of the $\epsilon''_{||}$ vs. f curves is the strong reduction in the maximum of the loss curve observed on going to the A_2 -phase.

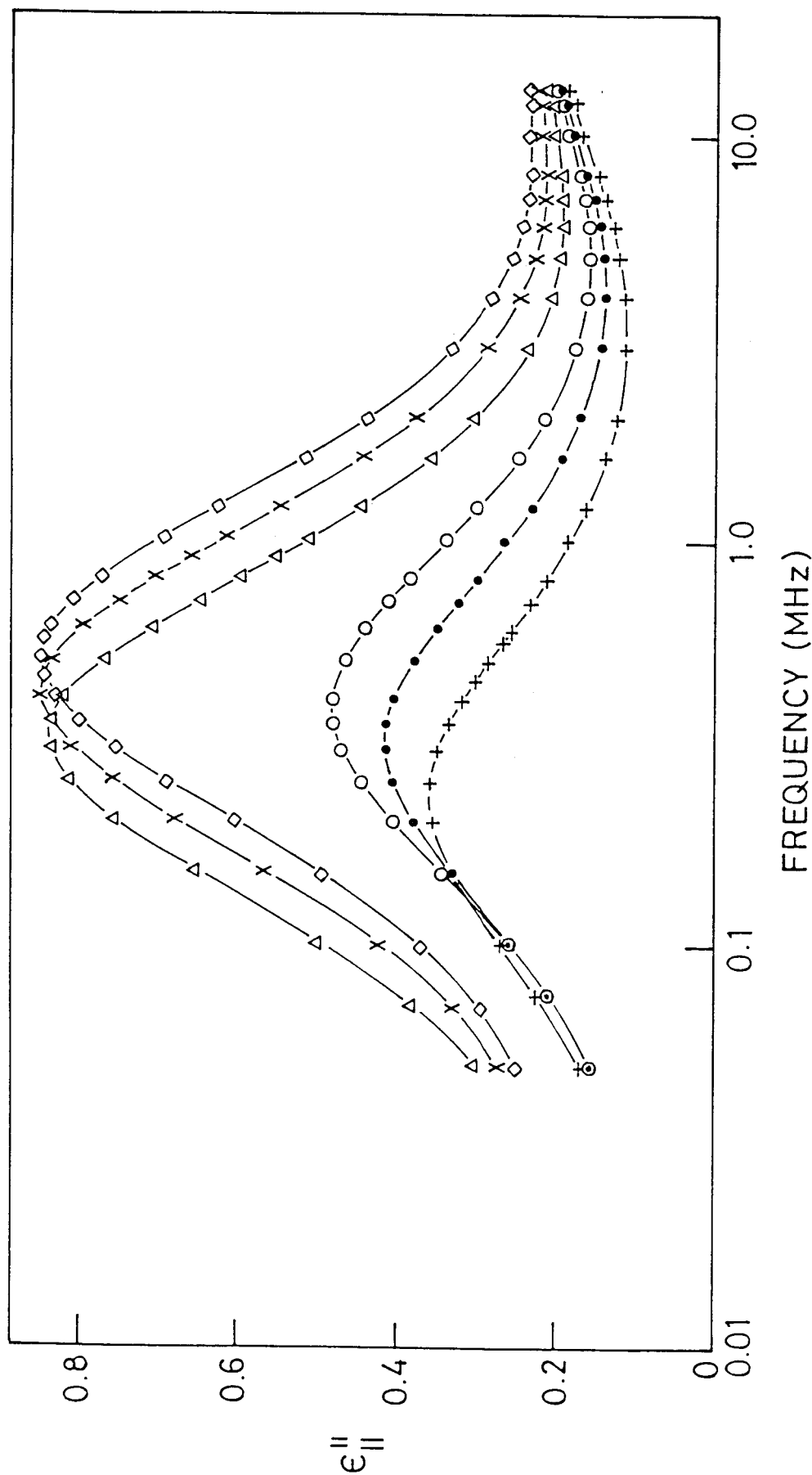


Figure 3.28. Representative loss curves of DB5CN in the nematic (◇ 153.5°C, × 149°C, △ 143.7°C) and smectic A₂ (○ 134.8°C, ● 129.6°C, + 122.9°C) phases.

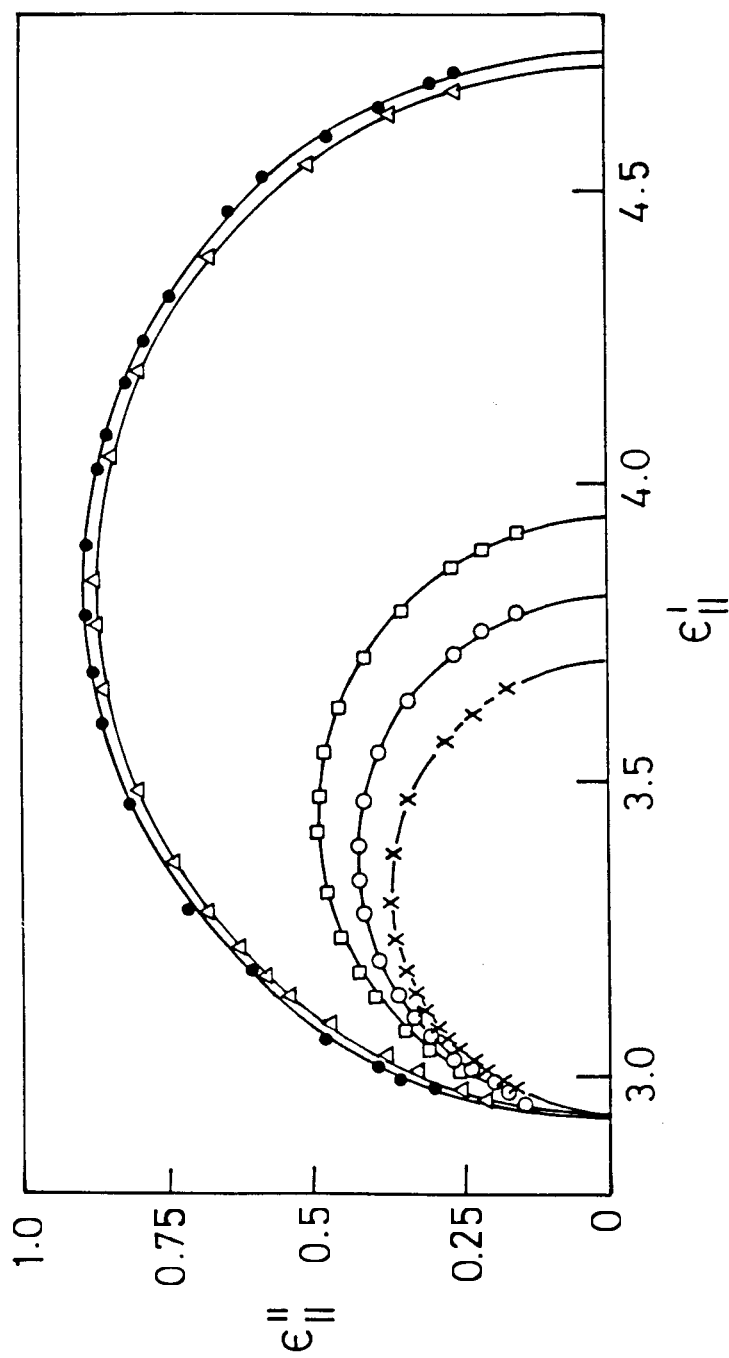


Figure 3.29

Representative Cole-Cole plots of DB5CN in the nematic (● 162.5°C, ▲ 143.7°C) and in the smectic A₂ (□ 134.8°C, ○ 129.6°C, × 122.9°C) phases.

The frequencies of relaxation f_R obtained from loss curves and Cole-Cole plots for a series of temperature are listed in Table 3.8. The plot of f_R vs. $1/T$ in the neighbourhood of N- A_2 transition is shown in Fig.3.30. The following important features are clear from this plot:

- 1 The activation energy in the A_2 phase (W_{A_2}) is less than the energy in N phase (W_N) while W_{A_2} was found to be substantially greater than W_N in the case of DB6CN, the higher homologue of DB5CN as reported by Druon et al.⁴⁵
- 2 There is a narrow range of temperature of about 4°C in which the data do not fit Arrhenius law. This seems to be the precursor effect of A_2 phase as we come from N phase. It is interesting to note from Fig.3.27 that $\epsilon_{||}$ also shows a drastic reduction in the same region of temperature over which the Arrhenius law is seen to break down in Fig.3.30.
- 3 Perhaps the most interesting feature of the dispersion result is that frequency of relaxation f_R in A_2 phase extrapolated to the transition temperature is greater than that in the N phase showing that the relaxation time τ_R is lower in A_2 phase than in N phase. This in turn would mean that the molecular reorientation is easier in the bilayer A_2 phase.

TABLE 38

Frequency of relaxation (f_R) as a function of temperature in
the nematic and smectic A_2 phases of DB5CN

S.No.	Temperature (°C)	Frequency of relaxation (in MHz)		Mean f_R
		From loss curve	From Cole-Cole	
<u>N P h a s e</u>				
1	159.7	0.760	0.760	0.760
2	158.6	0.720	0.713	0.717
3	156.2	0.625	0.630	0.628
4	154.2	0.600	0.595	0.599
5	153.9	0.597	0.599	0.598
6	151.6	0.530	0.524	0.527
7	149.8	0.495	0.490	0.493
8	147.0	0.413	0.415	0.414
9	146.8	0.430	0.428	0.429
10	146.0	0.410	0.408	0.409
11	144.9	0.395	0.400	0.398
12	144.2	0.375	0.378	0.377
13	143.0	0.360	0.358	0.359
14	142.2	0.345	0.347	0.346
15	140.2	0.320	0.323	0.322
16	139.9	0.315	0.317	0.316
<u>S m e c t i c A₂</u>				
17	139.0	0.330	0.333	0.332
18	138.0	0.425	0.416	0.421
19	136.1	0.440	0.436	0.438
20	134.1	0.430	0.433	0.432
21	132.0	0.385	0.379	0.382
22	130.2	0.360	0.361	0.361
23	129.4	0.355	0.356	0.356
24	128.2	0.335	0.332	0.334
25	125.0	0.287	0.282	0.285
26	124.2	0.275	0.272	0.274
27	122.5	0.258	0.260	0.259
28	121.4	0.245	0.244	0.245
29	120.2	0.230	0.232	0.231

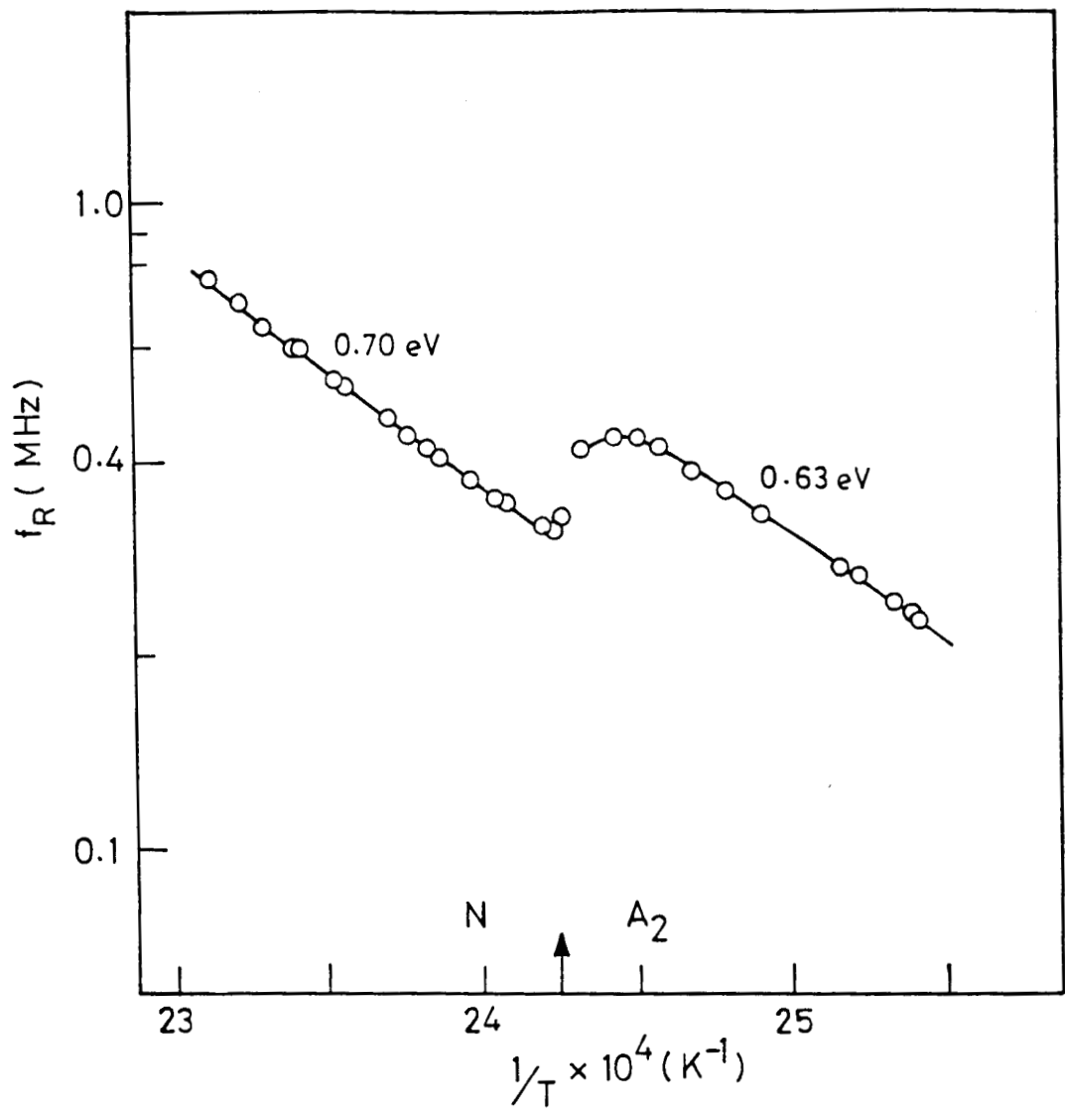


Figure 3.30

f_R versus $1/T$ plot of DB5CN in the nematic and smectic A₂ phases.

Thus our dielectric results on the A_2 phase of DB5CN do not show any evidence of the second dispersion which was predicted theoretically by Benguigui.⁴⁷ Further dielectric studies on other materials exhibiting the N- A_2 transition would be of considerable interest.

In conclusion, the dielectric properties near different kinds of N-A transitions have been studied. These studies show interesting differences in the behaviour of dielectric permittivities. A transition to the A_2 phase is accompanied by a very strong decrease in ϵ_{\parallel} . This reduction in ϵ_{\parallel} is attributed to the decrease in the effective dipole moment due to head-to-head arrangement of the neighbouring dipoles accompanying the formation of bilayer A_2 phase. In the case of N- A_I (polar) transition, the ϵ_{\parallel} shows a sharp decrease at the transition when the chain length is small but for higher value of n (n represents the number of carbon atoms in the alkyl chain), this change becomes less conspicuous. In N- A_d transition, there is a saturation of the antiparallel ordering as evidenced by the constancy of ϵ_{\parallel} with respect to the temperature throughout the A_d phase. Finally, in the case of non-polar monolayer phase, the behaviour of the static permittivity shows a continuous increase of $\Delta\epsilon$ with decrease of the temperature owing to an increasing trend of ϵ_{\perp} which is accompanied by the decreasing trend of ϵ_{\parallel} with decreasing temperature.

The dispersion data show that $W_N > W_A$ regardless of the type of the A phase. The non-polar substances seem to have highest value of W . An interesting jump in f_R is seen at N-A₂ transition while no such effect is observed near any other transitions. The f_R value in the A₂ phase very close to the N-A₂ transition is found to be greater than in the N phase indicating a reduction of the hindrance to the molecular reorientation about the short axis in the bilayer A₂ phase.

REFERENCES

- W.L.McMillan, Phys. Rev., **A4**, 1238 (1971)
- K.K.Kobayashi, Phys. Lett., **31A**, 125 (1970); J.Phys.Soc. Japan, 29, 101 (1970); Mol. Cryst. Liq. Cryst., 13, 137 (1971).
- W.Maier and G.Meier, Z.Naturforsch., **16a**, 262 (1961).
- L. Onsager, J. Chem. Soc., 58, 1486 (1936)
- N.V.Madhusudana and S.Chandrasekhar, Proc. Int. Liquid Crystals Conf., Bangalore, December 1973 - Pramana Suppl., 1, p.57; N.V.Madhusudana, K.L.Savithramma and S.Chandrasekhar, Pramana, **8**, 22 (1977).
- B.R.Ratna and R.Shashidhar, Pramana, 6, 278 (1976); B.R. Ratna and R.Shashidhar, Mol. Cryst. Liq. Cryst., 42, 113 (1977); C.Druon and J.M.Wacrenier, J. de Phys., 38, 47 (1977).
- 7 A.J.Leadbetter, R.M.Richardson and C.N.Colling, J. de Phys., 36, C1-37 (1975).
- 8 A.J.Leadbetter, J.C.Frost, J.P.Gaughan, G.W.Gray and A. Mosley, J. de Phys., 40, 375 (1979)
- 9 G.Sigaud, F.Hardouin, M.F.Achard and H.Gasparoux, J. de Phys., 40, C3-356 (1979)
- 10 F.Hardouin, A.M.Levelut, J.J.Benattar, G.Sigaud, Solid State Commun., 33, 337 (1980)

G.Sigaud, F.Hardouin, M.F.Achard and A.M.Levelut, *J. de Phys.*, 42, 107 (1981)

A.M.Levelut, *J. de Phys. Lett.*, 45, L603 (1984)

G.Sigaud, F.Hardouin, M.F.Achard, *Phys. Rev.*, **A 31**, 547 (1985)

B.R.Ratna, R.Shashidhar and V.N.Raja, *Phys. Rev. Lett.*, 55, 1476 (1985)

D.A.Dunmur, M.R.Manterfield, W.H.Miller and J.K.Dunleavy, *Mol. Cryst. Liq. Cryst.*, 45, 127 (1978)

C. Druon, J.M.Wacrenier, *Ann. Phys.*, 3, 199 (1978)

L.Bata and A.Buka, *Acta Physica Polonica*, **A 54**, 635 (1978)

H.Kresse, D.Demus and S.Konig, *Phys. Stat. Sol. (a)*, 41, K67 (1977)

C.Druon and J.M.Wacrenier, *Mol. Cryst. Liq. Cryst.*, 88, 99 (1982)

B.R.Ratna, R.Shashidhar and K.V.Rao, *Liquid Crystals, Proc. Int. Conf., Bangalore, December 1979*, Ed. S.Chandrasekhar (Heyden, London, 1980), p. 135

A.Buka, L.Bata, J.Szabon, *Mol. Cryst. Liq. Cryst.*, 103, 307 (1983)

G.Heppke, R.Hopf, B.Kohne and K.Praefcke, *Advances in Liquid Crystal Research and Applications*, Ed. L.Bata (Pergamon, Oxford, 1980), p. 141

- 23 G.Heppke, R.Hopf, B.Kohne and K.Praefcke, *Z.Naturforsch.*, **35b**, 1384 (1980)
- 24 H.Kresse, A.Wiegeleben, D.Demus, *Kristall and Technik*, **15**, 341 (1980)
- 25 A.Buka, L.Bata, H.Kresse, *Hungarian Acad. Sc., Budapest*, KFKI-1980-04
- 26 L.Bata, A.Buka, *Advances in Liquid Crystal Research and Applications*, Ed. L.Bata (Pergamon, Oxford, 1980), p.251
- 27 A.Buka, L.Bata, *Advances in Liquid Crystal Research and Applications*, Ed. L.Bata (Pergamon, Oxford, 1980), p.261
- 28 L.Bata, A.Buka, *Mol. Cryst. Liq. Cryst.*, **63**, 307 (1981)
- 29 H.Kresse, Ch.Selbmann, D.Demus, A.Buka, L.Bata, *Cryst. Research and Technology*, **16**, 1439 (1981)
- 30 J.Jadzyn and P.Kedziora, *Mol. Cryst. Liq. Cryst.*, **145**, 17 (1987)
- 31 G.V.Vani, *X-ray Analysis of the Crystal Structures of Some Mesogenic Compounds*, Ph. D. Thesis, University of Mysore, 1978
- 32 S.Torza and P.E.Cladis, *Phys. Rev. Lett.*, **32**, 1406 (1974)
- 33 J. Als-Nielsen, R.J.Birgeneau, M.Kaplan, J.D.Litster and C.R.Safinya, *Phys. Rev. Lett.*, **39**, 352 (1977)

- 34 R.Shashidhar and Geetha G. Nair (to be published)
- 35 P. Debye, 'Polar Molecules', Chern. Catalog Co. (1928)
- 36 A.J.Martin, G.Meier and A.Saupe, Symp. Faraday Soc., 5, 119 (1971)
- 37 C.Legrand, J.P.Parneix, A.Chapoton, Nguyen Huu Tinh and C.Destrade, J. de Phys. Lett., 45, L-283 (1984)
- 38 N.V.Madhusudana, B.S.Srikanta, M.S.R.Urs, Mol. Cryst. Liq. Cryst., 108, 19 (1984)
- 39 S.Chandrasekhar, Mol. Cryst. Liq. Cryst., 124, 1 (1985)
- 40 A. Oestreicher (Private communication)
- 41 R.Hopf (unpublished)
- 42 J.Thoen, G.Menu, Mol. Cryst. Liq. Cryst., 97, 163 (1983)
- 43 B.R.Ratna, "Dielectric Properties and Short Range Order in Liquid Crystals", Ph. D.Thesis, University of Mysore, 1978
- 44 L.Benguigui and F.Hardouin, J. de Phys. Lett., 42, L-381 (1981)
- 45 C.Druon, J.M.Wacrenier, F.Hardouin, Nguyen Huu Tinh and H.Gasporoux, J. de Phys., 44, 1195 (1983)
- 46 L.Benguigui and F.Hardouin, J. de Phys. Lett., 45, L-179 (1984)

- 47 L.Benguigui, J. de Phys., 44, 273 (1983)
- 48 R.M.Hornreich, M.Luban and S.Shtrikman, Phys. Rev. Lett.,
35, 1678 (1975)